



**THE OPTIMISATION OF HYDRODYNAMIC CAVITATION AS AN ADVANCED
OXIDATION OPTION FOR THE REMOVAL OF PERSISTENT CONTAMINANTS IN
WASTEWATER**

By NATACHA KABATA KAKAMA (215113942)

Thesis submitted in fulfilment of the requirements for the degree

Master of Engineering in Chemical engineering

in the Faculty of Engineering

at the Cape Peninsula University of Technology

Supervisor: Prof TUNDE V. OJUMU

Co-supervisor: Prof LESLIE F. PETRIK

Bellville campus

December 2022

CPUT copyright information

The thesis may not be published either in part (in scholarly, scientific or technical journals), or as a whole (as a monograph), unless permission has been obtained from the University.

Declaration of authenticity

I, **NATACHA KABATA KAKAMA**, acknowledge that the contents of this thesis is my own unaided work, and that the thesis has not previously been turned in for academic examination towards any qualification. In addition, it represents my own views and not necessarily those of the Cape Peninsula University of Technology.



Signed

Date 01 September 2022

Abstract

Wastewater is growing into a scarce commodity as more and more demand upon it in urban city is placed. The presence of persistent contaminant such as dye and perfluorinated compounds from industries is placing a demand on the need to design technique of removal of these chemicals from water as they induce adverse effects on life. This study investigated an approach to solving this problem of water scarcity using the hydrodynamic cavitation pilot plant. This work thus explores the application of the hydrodynamic cavitation plant combined with the venturi to suggest a way to clean water. The evaluation of the cost of implementation and investment was also explored. The study begun with the optimisation of the processes of removal by exploring the effect of orifices of size 2, 3, 4, 5 and 6 mm on the decolouration of orange II dye. The impact of catalyst: Iron II, oxidising agent: hydrogen peroxide, contact time were evaluated to suggest the ideal conditions under which the removal of perfluorooctanoic acid were to be removed from wastewater. It turned out that the decolouration of 20 ppm of orange II dye in simulated industrial textile wastewater was achieved at 90% efficiency under the following conditons: the pressure at the inlet was maintained at 300 KPa, the temperature at 34°C, the pH at 2 and the orifice size at 2 mm of diameter. The system had an energy efficiency of 38% or $1.36 \times 10^{-4} mg/J$ cavitational yield. The material as well as the energy balance showed the law of conservation was observed. The energy of the system was found to be 839 Watt. The kinetic study proved the decolouration reaction was pseudo first order and the rate of decolourisation of orange II was 0.23 min^{-1} . The total capital investment to acquire the HC pilot plant was R 27 305 and the total operating cost for a 10 L sample run on the HC pilot plant over a period of 10 min was R 8.82. The technique proved that the combination of venturi and orifice requires the throat size of the venturi to be similar or equal to that of the orifice for better efficiency.

Keywords

Advanced oxidation processes, hydrodynamic cavitation, persistent contaminants, dyes, perfluorinated compounds, wastewater

Acknowledgements

Thank you to

My spouse Mr **Wakwanyembo Eloge Lwamba** for his guidance, encouragement, dedication and support throughout this time of study. I appreciate our lovely daughter Faveur Grace Lwamba who was born during the course of this work. Such an amazing event.

My supervisors, professor **Tunde V. Ojumu and professor Leslie F. Petrik** for their guidance, their time and valuable suggestions throughout this research project. Above all, I thank them for offering me guidance, technical input, moral and financial support.

Dr Kassim Badmus, Miss Ninette Irakoze and Dr Emile Mouele have been very inspiring to me during these studies. They have guided, mentored me throughout the course of this work. My appreciation is also extended to each member of the Environmental and Nano Sciences research group.

Cape Peninsula University of Technology (CPUT) and their staff for an open door policy. I hold in high esteem the entire Chemical Engineering community at CPUT for forging us through this time. I appreciate The Cape Peninsula University of Technology for providing Research funds.

My parents **Pierre Andre Kakama Tiar Osia, Marie Therese Mungende Ndaienen**, my parents in-law **Guy Nyembo and Stephanie Masangu** for their prayers and encouragements. May my siblings Patrick, Sandra, Christian, Rachel, Olga, Dr. Aristide, Ruth, Yannick, Grace, Benita Kakama, my cousin Elyse Kimpiab and my friend Fabrice Kapiamba etc find here the expression of my appreciation.

Dedication

I dedicate this research work to the **Almighty God**, for helping me come out victorious. He has been faithful from beginning to end. I dedicate this work to my love and Husband **Wakwanyembo Eloge Lwamba**, to my lovely daughter **Faveur Grace Lwamba**, to my parents **Pierre Andre Kakama Tiar Osia and Marie Therese Mungende Ndaienen and to my siblings** for their support and love.

List of symbol and Glossary

Symbol	Description	Units
A	Area	m^2
D	Diameter	M
F	Friction loss	j/kg
f	Friction factor	No units
g	Gravitational acceleration	m/s^2
H	Enthalpy	J/kg
L	Length	M
k	Velocity head factor	No units
M	Mass	Kg
P	Pressure	Pa
T	Time	S
v	Velocity	m/s
\dot{V}	Volumetric flow rate	m^3/s
W_s	Shaft work	W
Z	Height	M
ϵ	Relative roughness	No units
ε	Absolute roughness	M
μ	Viscosity	Pa.s
π	Pi	No units
ρ	Density	Kg/m^3
α	Order of reaction	No units

Glossary

AOPs:	Advanced oxidation processes
BOD:	Biochemical Oxygen Demand
COD:	Chemical Oxygen Demand
Fe ²⁺	Ion (II)
HC:	Hydrodynamic Cavitation
H ₂ O ₂	Hydrogen peroxide
O2:	Orifice 2 mm diameter hole
O2V:	Orifice 2 mm diameter hole and venturi
O3:	Orifice 3 mm diameter hole
O4:	Orifice 4 mm diameter hole
O5:	Orifice 5 mm diameter hole
O6:	Orifice 6 mm diameter hole
OH:	Hydroxyl
POPs:	Persistent organic pollutants
Ppm:	Parts per million
TOC:	Total organic carbon
UV:	Ultra-violet
V:	Venturi

Table of contents

Declaration of authenticity.....	i
Abstract	ii
Keywords	iii
Acknowledgements	iv
Dedication	v
List of symbol and Glossary	vi
Table of contents	viii
List of figures	xii
List of tables.....	xiv
1. CHAPTER 1. INTRODUCTION	1
1.1 Background to the research problem	1
1.2 Problem statement	2
1.3 Aim and research objectives	2
1.4 Research questions	3
1.5 Significance of the research.....	3
1.6 Research approach	4
1.7 Scope and Delineation of the research.....	4
1.8 Chapter summary.....	4
2. CHAPTER 2. LITERATURE REVIEW	5
2.1 Wastewater	5
2.1.1 Wastewater treatment	5
2.2 Persistent contaminants.....	6
2.2.1 Dyes	6
2.2.2 Perfluorinated compounds.....	8
2.3 Methods of contaminants removal.....	10
2.3.1 Physical methods.....	10
2.3.1.1 Coagulation.....	10

2.3.1.2	Adsorption.....	11
2.3.1.3	Membrane filtration.....	11
2.3.1.4	Ion exchange dye removal technique.....	11
2.3.1.5	Irradiation removal technique	11
2.3.2	Biological methods	12
2.3.2.1	Aerobic and anaerobic methods.....	12
2.3.2.2	Enzymatic methods	12
2.3.2.3	Fungi culture	13
2.3.2.4	Microbial culture	13
2.3.2.5	Pure and mixed culture	13
2.3.3	Chemical methods	13
2.3.3.1	Ozonation	13
2.3.3.2	Oxidation	14
2.3.3.3	Electrochemical methods.....	14
2.3.3.4	Ultraviolet irradiation methods	15
2.3.3.5	Photochemical methods of degradation of dyes.....	15
2.3.3.6	Advanced oxidation processes	15
2.3.4	Hydrodynamic Cavitation	18
2.3.5	Hydrodynamic cavitation optimisation.....	19
2.3.5.1	Effects of geometrical parameters.....	19
2.3.5.2	Effect of Pressure and Cavitation number.....	20
2.3.5.3	Physicochemical proprieties of the liquid.....	20
2.4	Process evaluation.....	23
2.4.1	UV-Vis spectrophotometry	23
2.4.2	Material balance	23
2.4.3	Kinetic study: rate of reaction.....	23
2.4.4	Energy balance and energy efficiency of the HC pilot plant	24
2.4.5	Production cost.....	24
2.4.5.1	Estimation of capital investment cost.....	25
2.4.5.2	Factorial method.....	26

2.4.5.3	Total production cost and operating cost.....	27
2.5	Chapter summary.....	28
3.	CHAPTER 3. RESEARCH DESIGN AND METHODOLOGY	29
3.1	Experimental outline	29
3.1.1	Material	29
3.1.2	Apparatus	30
3.1.3	Experimental Set up.....	30
3.1.4	Experimental procedure	32
3.2	Data analysis	34
3.2.1	Material balance	34
3.2.2	Kinetics studies.....	34
3.2.3	Energy efficiency.....	36
3.3	Analytical methods	38
3.3.1	UV analysis	38
3.3.2	Chemical Oxygen Demand	39
3.3.3	pH-meter	39
3.3.4	Data analysis	40
3.4	Summary.....	41
4.	CHAPTER 4. RESULTS AND DISCUSSION	42
4.1	Optimization of hydrodynamic cavitation on dye removal.....	42
4.1.1	Effect of different cavitating devices on dye decolouration.....	42
4.1.2	The effect of orifice size on the presence of Iron sulphate and hydrogen peroxide	43
4.1.2.1	Removal of dye using 100 mg of Iron sulphate within 60 min	43
4.1.2.2	Removal of dye using 10 mL hydrogen peroxide (oxidising agent) within 60 min	44
4.1.2.3	Removal of Orange II using (Fenton reagents) within 60 min.....	46
4.1.2.4	Removal of Orange II using various orifices and venturi at 10 min	47
4.1.2.5	Observed Hydrodynamic Cavitation under optimised conditions	48
4.1.3	Removal of Perfluorooctanoic acid using optimum conditions	49
4.2	Material Balance.....	50

4.2.1	Material balance calculations.....	50
4.3	Chemical kinetics.....	52
4.4	Energy balance around HC pilot plant.....	55
4.5	Cost	59
4.5.1	Cost estimation calculations.....	59
5.	CHAPTER 5. GENERAL CONCLUSIONS AND RECOMMENDATIONS.....	62
	REFERENCE.....	64
	APPENDIX A.....	67
	APPENDIX B.....	80

List of figures

Figure 2.1 Chemical structure of Azo dye	7
Figure 2.2 Orange II.....	8
Figure 2.3 Structure of Perfluorooctanoic acid (Pramanik et al., 2015).....	9
Figure 3.1 Schematic diagram of removal of POPs.....	29
Figure 3.2 Hydrodynamic cavitation flow diagram schematic representation.....	30
Figure 3.3 Actual photograph of hydrodynamic cavitation pilot plant.....	31
Figure 3.4 Schematic representation of orifices cavitating device with 3mm thickness each	31
Figure 3.5 Actual photograph of orifices cavitating device.....	32
Figure 3.6 Schematic representation of the venturi cavitating device	32
Figure 3.7 UV Vis-spectrophotometer instrument.....	38
Figure 3.8 HACH DR/2010 machine (HACH, 2010)	39
Figure 3.9 UV-Vis Calibration curve for orange II dye	40
Figure 3.10 PFOA data measurement	41
Figure 4.1 Effect of different cavitating devices on dye decolouration in the HC pilot plant (Fixed parameters: Orange II concentration 20 ppm, 10 L solution volume, solution pH 2, 60 min experiment, 10 min sampling interval, 300 KPa inlet pressure, 22°C starting temperature ...	42
Figure 4.2 Effect of orifice size and catalyst (iron sulphate) on dye decolouration show O2, O3 and O4 had good decolouration efficiency.	44
Figure 4.3 Effect of orifice size in the presence of hydrogen peroxide on dye decolouration (Fixed parameters: Orange II concentration 20 ppm, solution volume 10 L, hydrogen peroxide 10 mL, solution pH 2, experiment run for 60 min, sampling interval of 10 min, inlet pressure of 300 KPa, starting temperature 22°C)	45
Figure 4.4 Effect of decolouration using orifice size 2, 3, 4, 5 and 6 in the presence of Iron sulphate and hydrogen peroxide showed that orifice 3 had the best removal and was followed by orifice 2. Orange II concentration: 20 ppm, solution volume: 10 L, Iron sulphate: 100 mg, hydrogen peroxide: 10 mL, solution pH: 2, experiment time: 60 min. The sampling interval of 10 min, inlet pressure of 300 KPa, starting temperature 22°C.....	46
Figure 4.5 Impact of different cavitating devices (orifice and venture) on dye decolouration in the HC pilot plant (Fixed parameters: Orange II concentration 20 ppm, solution volume 10 L, solution pH 2, experiment run for 10 min, sampling interval of 2 min, inlet pressure of 300 KPa, starting temperature 22°C.....	47
Figure 4.6 Effect of an orifice, a venturi and the combination of both cavitating devices on dye decolouration in the HC pilot plant (Fixed parameters: orifice 2 mm hole, Orange II	

concentration 20 ppm, solution volume 10 L, solution pH 2, experiment run for 10 min, sampling interval of 2 min, inlet pressure of 300 KPa, starting temperature 22°C)	48
Figure 4.7 Chemical oxygen demand results for Perfluorooctanoic acid (Fixed parameters: orifice 2 mm hole, PFOA concentration 20 ppm, solution volume 10 L, solution pH 2, experiment run for 10 min, sampling interval of 2 min, inlet pressure of 300 KPa, starting temperature 22°C)	49
Figure 4.9 Zero-order rate of reaction for removal of orange II using optimised conditions (Fixed parameters: orifice 2 mm, Orange II concentration 20 ppm, solution volume 10 L, solution pH 2, experiment run for 10 min, sampling interval of 2 min, inlet pressure of 300 KPa, starting temperature 22°C)	53
Figure 4.10 First order rate reaction plot for removal of orange II using optimised conditions (Fixed parameters: orifice 2 mm, Orange II concentration 20 ppm, solution volume 10 L, solution pH 2, experiment run for 10 min, sampling interval of 2 min, inlet pressure of 300 KPa, starting temperature 22°C).....	53
Figure 4.11 Second order rate of reaction plot for removal of orange II using optimised conditions (Fixed parameters: orifice 2 mm, Orange II concentration 20 ppm, solution volume 10 L, solution pH 2, experiment run for 10 min, sampling interval of 2 min, inlet pressure of 300 KPa, starting temperature 22°C)	54
Figure 4.12 Process flow diagram of HC reactor	55
Figure 4.13 Temperature rise profile (Fixed parameters: orifice 2 mm hole, Orange II concentration 20 ppm, solution volume 10 L, solution pH 2, experiment run for 10 min, sampling interval of 2 min, inlet pressure of 300 KPa, starting temperature 22°C)	57

List of tables

Table 2.1 Factors of direct and indirect cost items used for the estimation of the fixed capital cost (Sinnott, 2005).....	27
Table 3.1 Table of standards	29
Table 3.2 The table of instruments used	30
Table 3.3 Experimental details for optimisation of Hydrodynamic cavitation.....	33
Table 3.4 Absorbance measurement	40
Table 3.5 Chemical oxidation demand measurement.....	40
Table 4.1 Summary of the mole fraction of the component material balance around the tank	52
Table 4.2 summary of component material balance around the tank	52
Table 4.3 : Energy balance calculation constants	56
Table 4.4 Raw materials prices.....	60
Table 4.5 Utilities prices.....	61
Table 0.1 Table Absorbance measurements and percent decolouration of OR2 using orifice 2 mm diameter hole in the HC pilot plant at an inlet pressure of 300 kPa for 60 min.....	67
Table 0.2 Absorbance measurements and percent decolouration of OR2 using orifice 3 mm diameter hole in the HC pilot plant at an inlet pressure of 300 kPa for 60 min.....	68
Table 0.3 Absorbance measurements and percent decolouration of OR2 using orifice 4 mm diameter hole in the HC pilot plant at an inlet pressure of 300 kPa for 60 min.....	68
Table 0.4 Absorbance measurements and percent decolouration of OR2 using orifice 5 mm diameter hole in the HC pilot plant at an inlet pressure of 300 kPa for 60 min.....	68
Table 0.5 Absorbance measurements and percent decolouration of OR2 using orifice 6 mm diameter hole in the HC pilot plant at an inlet pressure of 300 kPa for 60 min.....	69
Table 0.6 Absorbance measurements and percent decolouration of OR2 using venturi the.	69
Table 0.7 Absorbance measurements and percent decolouration of OR2 + 100 g FeSO ₄ using orifice 2 mm diameter hole in the HC pilot plant at an inlet pressure of 300 kPa for 60 min .	70
Table 0.8 Absorbance measurements and percent decolouration of OR2 + 100 g FeSO ₄ using orifice 3 mm diameter hole in the HC pilot plant system at an inlet pressure of 300 kPa for 60 min.....	70
Table 0.9 Absorbance measurements and percent decolouration of OR2 + 100 g FeSO ₄ using orifice 4 mm diameter hole in the HC pilot plant at an inlet pressure of 300 kPa	70

Table 0.10 Absorbance measurements and percent decolouration of OR2 + 100 g FeSO ₄ using orifice 5 mm diameter hole in the HC pilot plant at an inlet pressure of 300 kPa for 60 min.....	71
Table 0.11 Absorbance measurements and percent decolouration of OR2 + 100 g FeSO ₄ using orifice 6 mm diameter hole in the HC pilot plant at an inlet pressure of 300 kPa for 60 min.....	71
Table 0.12 Absorbance measurements and percent decolouration of OR2 + 10 ml H ₂ O ₂ using orifice 2 mm diameter hole in the HC pilot plant at an inlet pressure of 300 kPa for 60 min .	71
Table 0.13 Absorbance measurements and percent decolouration of OR2 + 10 ml H ₂ O ₂ using orifice 3 mm diameter hole in the HC pilot plant at an inlet pressure of 300 kPa for 60 min .	72
Table 0.14 Absorbance measurements and percent decolouration of OR2 + 10 ml H ₂ O ₂ using orifice 4 mm diameter hole in the HC pilot plant at an inlet pressure of 300 kPa for 60 min .	72
Table 0.15 Absorbance measurements and percent decolouration of OR2 + 10 ml H ₂ O ₂ using orifice 5 mm diameter hole in the HC pilot plant at an inlet pressure of 300 kPa for 60 min .	72
Table 0.16 Absorbance measurements and percent decolouration of OR2 + 10 ml H ₂ O ₂ using orifice 6 mm diameter hole in the HC pilot plant at an inlet pressure of 300 kPa for 60 min .	73
Table 0.17 Absorbance measurements and percent decolouration of OR2 + 100g FeSO ₄ + 10 ml H ₂ O ₂ using orifice 2 mm diameter hole in the HC pilot plant at an inlet	73
Table 0.18 Absorbance measurements and percent decolouration of OR2 + 100g FeSO ₄ + 10 ml H ₂ O ₂ using orifice 3 mm diameter hole in the HC pilot plant at an inlet pressure of 300 kPa for 60 min.....	73
Table 0.19 Absorbance measurements and percent decolouration of OR2 + 100g FeSO ₄ + 10 ml H ₂ O ₂ using orifice 4 mm diameter hole in the HC pilot plant at an inlet pressure of 300 kPa for 60 min.....	74
Table 0.20 Absorbance measurements and percent decolouration of OR2 + 100 g FeSO ₄ + 10 ml H ₂ O ₂ using orifice 5 mm diameter hole in the HC pilot plant at an inlet pressure of 300 kPa for 60 min.....	74
Table 0.21 Absorbance measurements and percent decolouration of OR2 + 100 g FeSO ₄ + 10 ml H ₂ O ₂ using orifice 6 mm diameter hole in the HC pilot plant at an inlet pressure of 300 kPa for 60 min.....	74
Table 0.22 Absorbance measurements and percent decolouration of OR2 using the combination of orifice 2 mm diameter hole and the venturi in the HC pilot plant at an inlet pressure of 300 kPa for 30 min	75

Table 0.23 Absorbance measurements and percent decolouration of OR2 using the combination of orifice 3 mm diameter hole and the venturi in the HC pilot plant at an inlet pressure of 300 kPa for 30 min	75
Table 0.24 Absorbance measurements and percent decolouration of OR2 using the combination of orifice 4 mm diameter hole and the venturi in the HC pilot plant.....	75
Table 0.25 Absorbance measurements and percent decolouration of OR2 using the combination of orifice 5 mm diameter hole and the venturi in the HC pilot plant at an inlet pressure of 300 kPa for 30 min	76
Table 0.26 Absorbance measurements and percent decolouration of OR2 using the combination of orifice 6 mm diameter hole and the venturi in the HC pilot plant at an inlet pressure of 300 kPa for 30 min	76
Table 0.27 Absorbance measurements and percent decolouration of OR2 using orifice 2 mm diameter hole in the HC pilot plant at an inlet pressure of 300 kPa for 10 min.....	76
Table 0.28 Absorbance measurements and percent decolouration of OR2 using orifice 3 mm diameter hole in the HC pilot plant at an inlet pressure of 300 kPa for 10 min.....	77
Table 0.29 Absorbance measurements and percent decolouration of OR2 using orifice 4 mm diameter hole in the HC pilot plant at an inlet pressure of 300 kPa for 10 min.....	77
Table 0.30 Absorbance measurements and percent decolouration of OR2 using orifice 5 mm diameter hole in the HC pilot plant at an inlet pressure of 300 kPa for 10 min.....	77
Table 0.31 Absorbance measurements and percent decolouration of OR2 using orifice 6 mm diameter hole in the HC pilot plant at an inlet pressure of 300 kPa for 10 min.....	78
Table 0.32 Absorbance measurements and percent decolouration of OR2 using venturi in the HC pilot plant at an inlet pressure of 300 kPa for 10 min.....	78
Table 0.33 Absorbance measurements and percent decolouration of OR2 using the combination of orifice 2 mm diameter hole and the venturi in the HC pilot plant at an inlet pressure of 300 kPa for 10 min	78
Table 0.34 Temperature reading.....	79
Table 0.35 Chemical oxygen demand measurements of perfluorooctanoic acid	79
Table 0.1 Moody chart for determination of friction factor f (Beck & Collins, 2008).....	80

1. CHAPTER 1. INTRODUCTION

This chapter covers a brief background, the problem statement, the aim and objectives, the research questions, the significance and delineation of the research studies were presented.

1.1 Background to the research problem

Water is a vital resource of life on earth. Water is studied in hydrology and it is established therein that life, animals, flora and fauna on earth depends on it. "Water is life" (Abdel-Raouf et al., 2019). The use of water in traditional society wasn't much of a problem. Villages organised themselves along a riverbank and didn't need to recycle any water for daily use. The beginning of industrialisation and modernisation caused cities to organise in a way that water become a polluted resource that needs recycling due to the large amount of water used daily (Trojanowicz, 2020a). In fact, the presence of dyes and other organic persistent molecules effluent from industries in wastewater has induced pollution to the environment due to the toxic and bioaccumulative nature of dyes (Panda et al., 2020).

Water has to meet specific physical, chemical, and biological criteria that qualify it as suitable for drinking purposes and use in homes. Water used in household is discharged to collectors and carry along urine, shampoo, and all sorts of waste, etc. The same is observed in industries where water is used as a carrier in some processes as well as a carrier of waste toward effluent treatment plants. Since useable water has to meet strict requirements for it to be considered safe, any deviation from such properties can cause it to lose its quality; when this phenomenon is observed; water is known as wastewater. When releasing water into the environment, it is not reasonable to release it untreated, or not knowing the extent of its contamination. Failure to treat water has been recorded to have adverse effects on the environment (Akpor & Muchie, 2015). It is a fairly new concept brought about by clean water scarcity in cities. There are various techniques of treating and removing different types of contaminants from water depending on the contaminant based on whether they are degradable, biodegradable, pharmaceutical, etc. (Gadipelly et al., 2014).

Food industries produce contaminants that can easily be removed using physical, biological or chemical techniques. Wastewater removal concept is applied to organic molecules that are hard to remove by conventional techniques, those molecules are termed Persistent Organic

Pollutants (POPs) such as dyes that could be sourced from the textile industries (Abdel-Raouf et al., 2019).

A large amount of industrial effluent contains toxic and bio-refractory organic pollutants including dyes, aromatics compounds, phenolic compounds and chlorinated hydrocarbons. The different chemicals found in contaminated water result from many chemicals processed in the manufacture of textile, pharmaceutical, pesticides and petrochemicals. The side-products of manufacturing are discharged into the water resulting in significant water contamination. These compounds are not completely removed by conventional biological processes (Padhi, 2012). Different methods of contaminant removal have been employed to attempt their removal but unsuccessfully. So far the following techniques have been used to remove POPs including membranes processes, carbon bed adsorption, biological methods, electrochemical methods and oxidation using chlorination and ozonation. Some other advanced oxidation processes (AOPs) had a high research record. Many studies have covered the removal of organics contaminants over the last few years. This work will explore new ways of removing dyes in effluents from textile industries using Hydrodynamic Cavitation.

Although they provide successful results, most AOPs find limited application because of their design challenges at a larger scale and high cost. Therefore, a better AOP technique had to be suggested which provides benefits on efficient removal of POPs.

1.2 Problem statement

Most of the known persistent contaminants are capable of circumventing conventional water treatment techniques which are physical (filtration, coagulation), biological (aerobic and anaerobic) and chemical. Therefore, the failure of conventional treatment methods is apparent. Meanwhile, chemical techniques are more favourable, they remain a costly alternative due to the design constraints requiring a large-scale processing plant. Obtaining an alternative technique such as Hydrodynamic Cavitation (HC) could assist to meet the requirements of effective POPs removal such as efficacy and acceptably low operating cost.

1.3 Aim and research objectives

This technique aims at establishing whether Hydrodynamic Cavitation Technique could be a suitable chemical free technique for the elimination of POPs from industrial effluents. This

study will explore and suggest a route for optimisation necessary for the successful implementation of HC and also evaluate its efficiency through testing upon selected persistent compounds.

The objectives of this work include:

- Investigate the efficiency of single hole orifice of various diameters on the removal of selected POPs (dyes)
- Evaluate the efficiency of the venturi on the removal of selected POPs,
- Assess the efficiency of combined orifice single hole and the venturi on the degradation of selected POPs,
- Investigate the effect of operating variables such as contact time, catalyst, oxidizing agent and Fenton reagents,
- Evaluate the removal of selected POPs (perfluorinated compounds) using optimum conditions,
- Perform material and energy balances,
- Perform chemical kinetic of the removal of POPs using the HC pilot plant.
- Perform cost estimation

1.4 Research questions

The objectives listed above would be met by answering the following research questions:

- How can Hydrodynamic cavitation pilot plant be optimised?
- Does the cavitating device (venturi and orifice) and the contact time play any role in the efficiency of removal of persistent contaminants?
- Is the mass conserved throughout the system during the removal of POPs?
- Was the HC system cost-effective?
- What rate law is followed during the removal of contaminant in the HC system?

1.5 Significance of the research

This research is aimed at providing a treatment option to solve wastewater disposal challenges faced when dealing with effluents containing POPs from industries. The successful implementation and mastery of this technique will help address clean water scarcity concerns.

This work will help assess the efficiency of the HC pilot plant considering contact time and the best cavitating device. Therefore, this research attempts to provide data of optimum conditions considering HC as a suitable advanced oxidation for effective elimination of wastewater POPs.

1.6 Research approach

This study focuses on the optimisation of the processes of elimination of simulated wastewater POPs (Orange II dye and perfluorooctanoic acid) using a HC pilot plant. It was achieved by varying parameters such as orifice sizes alone, venturi alone, selected orifice combined to the venturi, use of catalyst and then the use of the oxidising agent on the orifice of various sizes. These combinations were done to assess the extent of removal of dyes using UV visible. The optimum conditions were used to attempt the removal of perfluorooctanoic acid from simulated wastewater. The impact of contact time was studied with respect to the selected condition. The evaluation of Chemical Oxygen Demand (COD) was employed to evaluate the removal of perfluorooctanoic acid from wastewater.

1.7 Scope and Delineation of the research

This study focuses on the optimisation of HC as an advanced oxidation option for the removal of POPs in simulated textile industry wastewater. It will also assess the efficiency of orifice single hole and/or venturi for the removal of selected POPs (dyes and PFCs). The impact of contact time and size of orifice of the cavitating device on the removal of the selected POPs and decolourisation of dyes contaminated wastewater will be studied. Dyes (orange II) and Perfluorinated Compounds (PFCs) such as Perfluorooctanoic acids (PFOA) are the target compounds in this work although water matrices may contain several pollutants. This is due to their abundant occurrence in the environment, wide use as well as the limited time frame to complete this research.

1.8 Chapter summary

The introductory chapter provides the background to the study, the problem statement, the aim and the objectives of the research. It also highlights research questions which will be addressed by the study, the significance of the study, the research approach as well as the delineation of the extent of study.

2. CHAPTER 2. LITERATURE REVIEW

Chapter 2 covers the work other researchers have done on water treatment, the removal of persistent contaminants in wastewater by different methods namely conventional methods, advanced oxidation processes particularly hydrodynamic cavitation, and its optimization.

2.1 Wastewater

Water is life. It is so only when it meets a set standard of quality. Not all types of water are suitable for use. Any deviations from the set water standard can make water unpleasant to use. This can be the description of wastewater. Wastewater represents water that has lost its physical, chemical and biological properties that would disqualify it for drinking. There are three main sources of wastewater : domestic, industrial and storm water runoff (Trojanowicz, 2020a). Storm water runoff wastewater includes any water collected from streets, or paved surfaces after rain. Domestic and industrial wastewaters are respectively coming from homes and industries. Domestic and storm water runoff water are thought to be easy to clean. This is no longer true with the evidence brought forward by recent research made available. In fact, pharmaceuticals are bio-accumulating so that they are hard to remove from domestic water (Ojemaye & Petrik, 2021). While this accumulation is minimum for domestic water, industrial waters contains more water persistent contaminants (Trojanowicz, 2020a).

2.1.1 Wastewater treatment

The treatment of wastewater is necessary for avoiding health-hazards and environmental degradation. Wastewater treatment is required before releasing water back into nature or re-using it. Effluent from different industries require different treatment due to the varying nature of the different water bed. Domestic wastewater contains trace elements, salts (inorganic), many different persistent carbonaceous compounds (organics), worms, microorganisms (biological waste). The mining industry's effluent would contain metals salts and acid that needs to be mitigated. A different treatment would be required for waste from the oil industries. This is true of any effluent. Therefore, the source of wastewater needs to be known for an appropriate treatment to be designed. The water in cities such as Cape Town is collected in the mountains and undergoes basic treatment which includes physical treatment (through filtration and sedimentation), mechanical treatment (filtration); chemical treatment (pH

adjustment), and biological treatments with bacteria (Badmus et al., 2018). Some hard-to-remove substances in each category could include dyes, nanoparticles, heavy metals, and pharmaceutical products, for which a general technique of removal is not efficient (Abdel-Raouf et al., 2019).

2.2 Persistent contaminants

Persistent contaminants are chemical compounds that are difficult to remove from water. They resist degradation by chemical, photochemical or biochemical reactions in water (European Union Policy, 2017). Persistent contaminants have a long life span and stability during transport. In fact, they are semivolatile and can withstand several evaporation cycles, but they can be air-lifted so that they can easily be condensed. These compounds undergo bioaccumulation in living tissues. The majority of persistent compounds are water-soluble, they are toxic at low concentrations both to living organisms and the environment (Mustereț & Teodosiu, 2007). Persistent contaminants are found to induce diseases such as cancer, central nervous problems, reproductive disorders, disruption of an immune response (Badmus et al., 2018).

The majority of persistent contaminants are generated in chemical industries including the textile industry, pharmaceutical industry, chemical industry, paper industry, metallurgical industry, mining industry, petrochemical industry, etc. (Mustereț & Teodosiu, 2007). Wellness and health products have contributed a lot to pollution in water including hormones, pesticides, perfluorinated compounds (PFCs), persistent organic pollutants (POPs). The European Union has drafted standards to regulate and limit the number of persistent contaminants, in the environment through the Stockholm agreement by limiting the number of imports or exports of products that present a health hazard to the environment (European Union Policy, 2017), (Macoveanu et al., 1997).

The need for clothes is universal. Clothes and textiles are made in industries using many colouring agents and other chemicals among which are dyes and perfluorinated compounds. Both of these compounds have been described as persistent contaminants and are difficult to remove from wastewater using conventional processes.

2.2.1 Dyes

Dyes are organic molecules with unsaturated bonds that can absorb a fraction of UV light and emit the rest. The unsaturation of the chemical structure of a dye gives it the benefit of emitting colour (Benkhaya et al., 2020). Dyes have been known for over 4000 years. Early dyes were obtained from nature and presented no ill effect as a result of their inherent ability to be less toxic and be easily biodegradable. The latest dyes are made synthetically and have a much better colouring ability which depends on the substituting functional groups that generally are Azo groups (-N=N-), nitro groups (-NO₂), nitroso (-N=N-) etc. These unsaturations are responsible for absorbing light in the UV region between 380 and 750 nm. Dyes have been used in clothing for the ability to convey their colour to the fabric to which it is applied (Benkhaya et al., 2020).

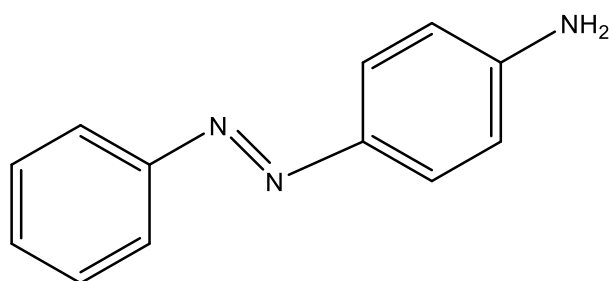


Figure 2.1 Chemical structure of Azo dye

Dyes are one of the greatest persistent environmental contaminants. They are widely used for colouring various products. Natural dyes were used earlier, but they revealed low colour fastness when subjected to washing and sunlight. A wide diversity of dyes that are very effective and brighter have been introduced through the discovery of synthetic dyes made in 1856 by W. H. Perkins (Mustereț & Teodosiu, 2007). While some dyes are classified based on functional groups, others are classified as a function of the structure of chromophores (absorbing section of the dye), Azo dyes are the most common due to their cost-effectiveness and simplicity of synthesis (Benkhaya et al., 2020).

Azo dyes are used in paper printing, textile dyeing, cosmetics, food industries, pharmaceutical polymers, paints and petroleum products as an additive. Berradi (2019) reported that the global usage of dyes was 700 000 tonnes with a third of this quantity consumed by textile industries. Berradi (2019) reported 25 mg/L of dyes have been reported in textile industries effluents. The presence of azo dyes in textile effluents causes intense colouring and induces an opacity of rivers to sunlight and an oxygen deficiency in the effluent, by stopping photosynthesis, and causes the death of aquatic lives (Berradi et al., 2019). Compounds such as aromatic amines

generated by the reduction of coloured reagents are carcinogenic and mutagenic. They reach humans organs through the consumption of fish from contaminated effluent which bioaccumulates dyes in certain tissues. Skin irritation can occur when dye effluents come in contact with skin (Saranraj 2013; Akhtar et al. 2016).

Orange II is one of the most common azo dyes found in textiles and its structure is depicted in Figure 2.2. It makes up 75 % of textiles dyes. Its wide application is due to its use at a low temperature (60°C) compared to most azo-free dyes requiring a temperature of up to 100°C.

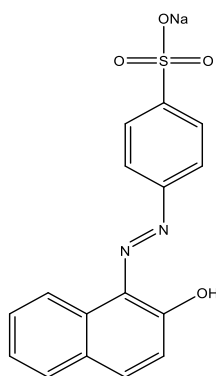


Figure 2.2 Orange II

Several techniques for dye decolourisation and removal from waters and wastewaters have been developed to reduce their presence in the environment. These methods are classified as physical, biological and chemical. Each method has its advantages and drawbacks and will be discussed in section 2.3.

2.2.2 Perfluorinated compounds

Perfluorinated compounds (PFOs) are organic pollutants in which fluorine atoms have replaced some hydrogen atoms. Their carbon chains are of different lengths such as C6 to C14 (Kunacheva et al., 2011). They have been reported as a global issue due to their role in the many recorded human and animal deaths. They have been used in surfactants, firefighting foams, protective coatings. Their use has been reported also in textile, pulp and paper industries, packaging industries, etc. These compounds include compounds such as Perfluorooctanoic acid (PFOA) and perfluorooctane sulfonic acid (PFOS) and are known as the Perfluorinated compounds (PFCs). Their nature has made them suitable for use in food packaging including boxes and plastics (Kunacheva et al., 2011). They have been reported to cause cancer and this makes them a source of concern as materials used next to food. Due

to the impacts of their action on the environment; their use, importation and exportation have been regulated in Europe (European Union Policy, 2017).

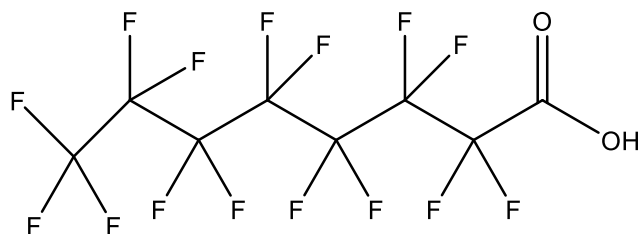


Figure 2.3 Structure of Perfluorooctanoic acid (Pramanik et al., 2015)

Traditional contaminants were simple molecules, non-polar, lipophilic and non-aromatic. The recorded emerging contaminants belong to more sophisticated classes of compounds. They are polar, show little volatility and little biodegradability. Their varying structure is the reason they are found in more places including in living animals where they bioaccumulate. PFOS can form by degradation of larger molecules or biodegradation in living organisms. Recent research has reported their presence in domestic water, surface water, groundwater, etc. (USEPA, 2017). Since the greatest challenge remains their resistance to removal, the following lines will explore the possible route of removal.

The quantitative evaluation of the perfluorinated compounds includes the monitoring of both the chemical oxygen demand (COD) and the biochemical oxygen demand (BOD). The relative measurement of both can be used to draw conclusions on the degree to which the degradation of organic materials in wastewater occurs. The BOD evaluates the amount of oxygen consumed by biological organisms and the COD express the amount of oxygen in wastewater required to totally oxidise chemically organic compounds and minerals in waste water to inorganic materials (Prambudy et al., 2019). The removal of perfluorinated compounds from wastewater is monitored using the amount of chemical oxygen demand (COD) in solution in mg/L. The acceptable limit of removal of PFOA in South Africa has been limited to below 30 mg/L COD by government and can vary from one country to another. The chemical oxygen demand (COD) is a measure that can be used to monitors the amount of PFOA in a solution (Vítez et al., 2012). A high level of COD can cause a lack of oxygen in wastewater causing serious damage to the environment. The reduction of COD can be achieved by adding a strong oxidising agent such as hydrogen peroxide to the sample which degrade organic compounds.

2.3 Methods of contaminants removal

Kant (2012) suggests the following three classifications of removal techniques depending on the type of contaminants and effluent namely physical, chemical and biological. The physical method includes, filtration, sedimentation, floatation, foam fractionation coagulation, reverse osmosis, solvent extraction ionization, radiation, incineration, adsorption, distillation membrane treatment. The biological method includes stabilisation, activated sludge, anaerobic digestion, fungal treatment, flocculation and finally, the chemical method includes neutralisation, catalysis, reduction, oxidation, electrolysis and ion exchange (Kant, 2012).

2.3.1 Physical methods

Physical methods of removal of contaminants are simple processes that occur with no change in the inherent nature of the species undergoing the process. After the process has been completed, the nature of the object remains the same. It would include processes such as targeted substance coagulation, flocculation, adsorption, membrane filtration, ultra-filtration, nanofiltration, reverse osmosis, sedimentation, flotation, extraction, ion exchange, and irradiation. These techniques are briefly discussed below (Malato, 2008).

2.3.1.1 Coagulation

Coagulation is used together with flocculation to precipitate the targeted contaminant using coagulant species such as aluminium, salts, and iron salts. Coagulation is good for the removal of insoluble dyes, but it is ineffective for the removal of reactive and acid dyes. Furthermore, the application of this process is limited due to the low colour removal efficiency and generates a large amount of sludge requiring extra costs for its treatment (Pramanik et al., 2015). Coagulation can be achieved by sedimentation or gravity settling. It is a process in which physical precipitation of particles occurs at the bottom of the container as a result of increased mass or instability of particles in solution (Kant, 2012).

Flocculation offers the benefits of being a cost-effective technique. It is easy to implement and is known for being robust. It is suitable for substances that are dispersed such as sulphur and vat dyes. However, it can be highlighted that a huge amount of contaminated sludge is generated in flocculation, it is not recommended for acids, azo, reactive dye effluents (Saratale et al., 2011).

2.3.1.2 Adsorption

Adsorption is a technique used to attach a substance to a surface using a material called an adsorbent. Adsorbents such as activated carbon, polymeric resins, fly ash, peat, and ion exchangers for dye can be good adsorption agents. Activated carbon is the most efficient adsorbent used with many types of dyes. Adsorption is simple and effective for the removal of various types of dyes (Kant, 2012). Most adsorbents are easily regenerated. Adsorption is costly and limited by the formation of a contaminated sludge (Katheresan et al., 2018).

2.3.1.3 Membrane filtration

Filtration using membranes is a method in which solid particles are separated from liquid by means of a sieve or a membrane with extremely small pores. Dyes have also been separated from clean water using this technique. POPs that have been coagulated can cause fouling of the membrane. This technique has a high efficiency of removal. Membranes are costly to maintain, requiring use of pumps to achieve high pressure. Membrane filtration like nano-filtration, ultrafiltration membranes, and reverse-osmosis remove all types of dyes from effluent. It is less used for being costly to maintain and operate. Also, the fouled membrane needs cleaning and regeneration (Kant, 2012).

2.3.1.4 Ion exchange dye removal technique

This technique is based upon the ability of a foreign ion to replace the dye molecule ion so that it is easily replaced from the flowing wastewater onto some solid ion exchange stationary phase.

It is a reversible process therefore; the ion-exchanger stationary phase can be regenerated to save cost. This technique produces high quality water. The technique is specific to a limited amount of dyes. But here too, the ion exchange will need regeneration (Katheresan et al., 2018).

2.3.1.5 Irradiation removal technique

Radiation can be used to eliminate dyes in solution. It is an effective technique for small scale removal and generally implemented for laboratory use. Experiments have revealed that the

technique implies formation of free radicals in solution that can oxidize the dye (Katheresan et al., 2018).

2.3.2 Biological methods

Biological methods include techniques that utilize some living organisms in the process. It is reputable for being a safe method. However, the technique limitation is the inability to determine accurately the growth rate and reaction kinetics (Pereira & Alves, 2012). The common technique in biology includes anaerobic, aerobic, enzyme degradation, fungal culture, algae degradation, microbial biomass, microbial cultures (mixed bacteria), pure and mixed cultures but microbes are fussy and easily die when the conditions are not favourable (Katheresan et al., 2018).

2.3.2.1 Aerobic and anaerobic methods

Anaerobic and aerobic methods are known as conventional biological methods for removal of nutrients. They are reputed for being inexpensive and simple techniques performed to break down a prepared sludge. This technique often comes before the discharge of dye effluents to the environment. It is able to decolourise a variety of dyes molecules. It is good to mention that this technique does not completely remove dye from wastewater. A drawback is that methane and hydrogen sulphide are formed as by-products. It requires a significant amount of time and wide open space. It is not suitable for all types of persistent contaminants (Saratale et al., 2011).

2.3.2.2 Enzymatic methods

Enzymatic methods degrade dye wastewater with extracted enzymes. Enzymatic methods such as white rot fungi are low-energy techniques and they are not harmful to the environment. They can be used over a wide pH and temperature range. However, dye molecules are often non-biodegradable by biological methods due to the structure of their molecules. Also, biological activity in liquid state fermentation is unable to eliminate dyes continually from wastewater. This is since the fermentation process and decolourisation demand residence time, hence, wastewater has to be kept in large tanks for the process (Chiong et al., 2016). The enzymatic technique is non-toxic and is cheap due to the ability of enzymes to be

regenerated. However, the production of enzymes is limited to small quantities (Katheresan et al., 2018).

2.3.2.3 Fungi culture

Fungi culture is a method through which dyes are broken down and consumed by fungi for self-growth. This technique is non selective and is suitable for the removal of a mixture of more than one dye. The technique needs time and nitrogen atmosphere. It often requires reactors to fast track the complete removal of dyes. The system is not easy to monitor in relation to its stability (Pereira & Alves, 2012).

2.3.2.4 Microbial culture

Microbial culture is a mixed technique in which the removal of dyes occurs as a result of synergic effects of both microbes and chemicals or bacteria. The technique needs over a day to achieve decolouration of dye wastewater which is considered fast. This technique is good for a short residence time and is cost effective when a large scale application is done (Katheresan et al., 2018).

2.3.2.5 Pure and mixed culture

The removal of dyes is achieved by using a mixture made up of algae, bacteria or fungi in presence of some chemicals. The technique is reusable and suitable for the removal of azo-dye. it however generates toxic colourless side-products and sludge. The technique would need additional water treatment making it expensive (Katheresan et al., 2018).

2.3.3 Chemical methods

Chemical methods used to treat dyes are methods using oxidising principles to remove dyes. Conventional dye removal methods include ozonation, electrochemical destruction, photochemical and ultraviolet irradiation, oxidation, Fenton reaction dye removal, Advanced Oxidation Process (Pereira & Alves, 2012).

2.3.3.1 Ozonation

Ozonation is an oxidation process in which ozone yielded from oxygen is used in the breaking down of conjugated double bonds of the chromophore leading to decolourisation. There are some advantages of ozone such as strong decolourisation ability for various dyes, it can be used in its gaseous state, hence does not expand the volume of wastewater or sludge. However, ozone is limited due to the low removal of COD (Chemical Oxidation Demand), disperse and insoluble dyes thus effluents still contains toxic degradation intermediates, its short half-life requires continual use hence making it an expensive process, it requires high pH (Tao et al., 2016), Surpăţeanu and Zahara (2004) showed that the decoloration was achieved using both UV and oxidation to cause the removal of acid red azo-dye. The efficiency of this technique was subject to hydrogen concentration, iron catalyst and the best result were obtain in acidic and neutral medium (Surpăţeanu & Zaharia, 2004).

2.3.3.2 Oxidation

Oxidation is a chemical method which use oxidising agent such as hydrogen peroxide to break down dye in effluents. The degraded organic molecules generate water and carbon dioxide (Katheresan et al., 2018). The use of a catalyst essentially enhances this process. This technique can completely degrade dyes in a reaction that is shorter compared to a decolouration reaction using no oxidising agent, but it is costly and requires pH control and activation of hydrogen peroxide agent. The technique needs catalysts such as iron II for better decolouration efficiency (Gogate & Bhosale, 2013).

2.3.3.3 Electrochemical methods

Electrochemical oxidation is a method that has a strong ability of breaking up organic compounds. This method involves electrocoagulation and electro-oxidation which are relevant to remove many contaminants. The electrochemical technique consists in passing an electric current between electrodes trigger a chemical response. The dyeing equipment is connected to the electrochemical cell with a non-soluble anode and electrochemical process strongly reduce the dye soak. Many factors affect electrochemical degradation including current intensity, number and spacing of electrodes used, pH, temperature, nature of electrolytes, surface tension, flow rate of wastewater and the properties of the dye are the elements influencing electrochemical degradation of dyes. This method performs a high degree of decolourisation, generates non-toxic products and no sludge, requires low temperature and no extra chemicals. However, it does not involve a high COD reduction and the main limitation is the high cost of electricity (Patients et al., 2012).

2.3.3.4 Ultraviolet irradiation methods

Ultraviolet irradiation constitutes a process through which dyes are decomposed generally in water by means of UV-light. This technique produces no sludge. However, It has been reported to be costly in energy and limited because of extended treatment time, it is slow, it does not penetrate dirty water, it leaves toxic intermediates (Katheresan et al., 2018). When combined with some alternative technique such as ultrasound, its performance has a much higher yield with almost no toxic side-products (Gore et al., 2014).

2.3.3.5 Photochemical methods of degradation of dyes

Photochemical methods of degradation of dyes is achievable because dyes are light sensitive. In this method, the ionisation of dyes is caused by the absorption of photons by dyes. The application of UV alone is not effective for the decolouration of dye. However, the combination of UV and H₂O₂ has a high colour removal technique (Pereira & Alves, 2012). Fenton reaction can be combined with UV radiation and remove dyes from wastewater. The technique is effective. It produces no sludge. However, it is costly and produces many side products (Katheresan et al., 2018).

2.3.3.6 Advanced oxidation processes

Advanced oxidation processes (AOPs) are an alternative to conventional methods. They are techniques in which hydroxyl (OH) radicals are produced to oxidise various types of organic pollutants. There are several types of techniques in AOPs namely Fenton oxidation, photo Fenton, ozone/ UV oxidation, ozone/hydrogen peroxide oxidation, UV/hydrogen peroxide oxidation, ozone/ UV/ hydrogen peroxide oxidation, nano-zero valent ions, cavitation (Patil et al., 2014).

Dyes degradation using Fenton reagents employs a Fenton reagent made up of a mixture of catalyst and hydrogen peroxide respectively Fe²⁺ and H₂O₂. It is suitable for both soluble and insoluble dyes. It is also compatible for samples with solid contents. The Fenton technique is very efficient at removing colour, organic pollutants and chemical oxygen demand (COD), Fenton processes requires no input in energy The technique showed a low efficiency for fat and dispersed dyes. The technique generates a high quantity of iron sludge at low pH value

(Badmus et al., 2018). The technique is pricy and works only for a narrow pH value and generates a high volume of sludge:

The general equation that summarises the Fenton process can be expresses as follow:



Zero-valent iron technique is a Fenton process technique based upon the use of zero valent iron. It produces less sludge. It is much more effective than Fenton and can be combined to other metals playing the role of catalyst. However, the technique makes the stability of nanoparticles to be questionable (Chakinala et al., 2009).

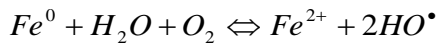
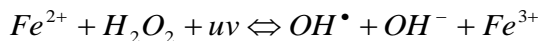


Photo Fenton make use of the same reagent as Fenton oxidation. UV radiation is added to the process. It is more efficient than Fenton oxidation due to the presence of UV radiation and is pricier than physical methods (Kumar et al., 2018). The following reaction summarises this process:



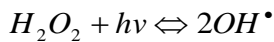
These next methods are all combined advanced oxidation techniques

Ozone/ UV, Ozone/ H₂O₂ oxidation,

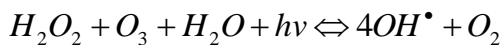
Ozone/ UV oxidation is a technique of dye removal employing the combination of both ozone and UV radiation in its processes (Sharma et al., 2011). The technique is very effective for heavily polluted samples and occurs in the open according to the reaction catalysed by sun rays as follow: ($O_3 + hv + H_2O \Leftrightarrow 2OH^\bullet + O_2$). The same technique gets more effective as a removal process when ozone and the oxidising agent (H₂O₂) in the degradation of organic pollutants are used. This technique is as efficient as photo Fenton oxidation technique. The oxidising agent (H₂O₂) combined helped make the technique very efficient. The technique consumes a lot of chemicals such as hydrogen peroxide and it is costly. It occurred according

to the following reaction: $2O_3 + H_2O_2 \Leftrightarrow 2OH^\bullet + 3O_2$. This technique offers the benefits of treating a large variety of contaminants (Abdel-Raouf et al., 2019).

UV/ Hydrogen peroxide oxidation technique involves the use of the hydrogen peroxide in the presence of light according to the reaction below. The technique is very efficient because the peroxide is decomposed in the presence of light into OH radicals. The amount of radicals generated is highly dependent on light intensity. This technique is selective of contaminants and requires high cost of treatment (Li et al., 2018).



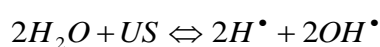
Ozone/ Hydrogen peroxide oxidation UV technique. Hydroxyl radicals are generated through the reaction between water and ozone, peroxide and iron II. The following reactions show the generation of OH. The technique is not cost effective and require the use of many chemicals (Sharma et al., 2011).



Cavitation is technique designed for treating complex wastewater containing persistent contaminants. Its usefulness is based on its ability to continuously generate hot spots and highly reactive free radicals without needing to add any additional chemical to the system. Once the condition of high temperature/low pressure, intense turbulence and liquid rapid motion is achieved; a chemical transformation is initiated with the main consequence of inducing dissociation and destruction of complex organic pollutants (Bagal & Gogate, 2014).

Cavitation techniques are classified based on various methods of energy generation. They are known as particle, optic, acoustic and hydrodynamic cavitation. Cavitation using elementary particle beams such as neutrons has been termed *particle cavitation*. In the event when high intensity photons are used to rapture the liquid continuum and achieve cavitation generation, the technique employed is known as *optical cavitation*. Some other means of achieving cavitation has involved the variation of sound waves in liquid solution at a frequency range between 16 KHZ to 100 MHZ, this has been known as *acoustic cavitation* (Saharan et al., 2012). The last technique known in this category is *hydrodynamic cavitation* and it is suitable to use.

Among the various modes of generating cavities (bubbles) in water given above, acoustic and hydrodynamic cavitation are easy to use and have thus been widely reported for their academic and industrial use. Hydrodynamic cavitation uses changes in fluid velocity of samples to generate bubbles (Gogate et al., 2006). Acoustic or ultra-sonicator technique generates bubbles as a result of pressure drop caused by sound waves generated by the sonicator. The technique is nontoxic with no side products. It requires almost no chemicals. This technique works better at small scale but is a high cost treatment. The following chemical reaction sums up the ultra sonicator chemical reaction (Gogate, 2007).



2.3.4 Hydrodynamic Cavitation

Hydrodynamic Cavitation (HC) has been studied extensively in the field of wastewater treatment by many researchers during the past decades (Badmus et al., 2020). It has been reported to be energy efficient and easy to upscale for the treatment of industrial effluents. The use of HC technique toward the removal of persistent organic pollutants (POPs) is common in textile, pharmaceutical, pesticide industries, and food industries. Hydrodynamic cavitation method revealed positive results in the degradation of bio-refractory pollutants (Chakinala et al., 2008).

Cavities (bubbles) are generated in HC as liquid flows through a constriction built in the design of the HC pilot plant. The common constrictions used are, (and not restricted to) venturi, orifices and throttling valve etc. As liquid goes through the constriction, a drop in pressure and heat is noticed increasing kinetic energy as the boiling point of the solvent decreases and vapour pressure builds up forming more bubbles. In fact, the pressure at the constriction gets lower than the liquid pressure favouring cavity formation (Lalwani et al., 2020). The formed cavities induce the formation of a pressure that can rise to as high as 1000 atm and a temperature of 10000 K. In this state, a chemical reaction results, breaking the hydrogen bond so that the water molecules dissociate and forms free OH radicals which oxidise organic pollutants as they come into contact. The extent and the number of cavitation events can be controlled by the number of constrictions designed in the HC pilot plant (Saharan et al., 2011).

Cavitation is a temporary process that is short-lived. In fact, as the liquid flows pass the constriction, the liquid pressure comes back to its original value. A phenomenon known as collapse of cavities is observed (Braeutigam et al., 2010). Cavitation can be achieved in various ways. In the case of a physical change induced cavitation, it would cease when stopping the cause that induced the change.

2.3.5 Hydrodynamic cavitation optimisation

Optimisation of HC is the action of making the best or most out of the device. The operating conditions such as the geometrical parameters, the inlet pressure, and the physicochemical properties of the liquid play an important role in the HC performance (Panda & Manickam, 2019). Therefore, adjusting their parameters in a way that better results are obtained for the least input is the aim of optimisation. The improvement of the efficiency of the HC depends on the following factors:

2.3.5.1 Effects of geometrical parameters

The design of the HC pilot plant defines the geometry and the number of times the constrictions re-occur. The section area at the throat, the ratio of the height to the length at the constriction, the divergence angle of downstream section in the venturi plays a defining role in the efficiency of the system (Innocenzi et al., 2018). The cavitation yield is also affected by the free area of the flow at the orifice of the reactor. The size of the generated cavity as well as their collapse is a function of all these parameters. For example, a device yields the maximum size of cavities for small angles of divergence. This occurs as a result of lower pressure of the flowing liquid during the constriction. Small cavities are obtained for large divergence angle due to a drastic fall in pressure during formation at the constriction. Hence, smaller divergence angle are preferred for their maximum sized cavity or their high cavitation output of OH[•] radicals (Lalwani et al., 2020). For the same pressure, a large inlet diameter of a HC pilot plant with small number of holes has proven to be more favourable to cavitation life span (Gogate, 2007).

Tao defines orifice using two parameters namely α and β . They are given by $\alpha = \frac{n\pi d_n}{n\pi(\frac{d_n}{2})^2}$ and

$\beta = n(\frac{d_n}{d_p})^2$ relationship in which n , d_n and d_p are respectively the number of holes, hole diameter and pipe diameter. For defined flow area, any increase in α and decrease in β causes the rate of removal of pollutant to increase (Tao et al., 2016). The formation and collapse of bubbles are more significant in orifices than in venturis. This can be attributed to the pressure

drop which is much higher in an orifice than in the venturi (Saharan et al., 2011). Cavitation intensity is greater in venturi than in orifices. This can be attributed to the smooth recovery pressure in the venturi downstream as a result of growth of cavities to maximum size whereas in the orifice, pressure recovers immediately as a result of short-lived cavities generated (Panda et al., 2020).

2.3.5.2 Effect of Pressure and Cavitation number

The pressure at the inlet and the number of cavitation events in the reactor determine the intensity of cavitation at the constriction. A high pressure at the inlet favours cavitation at a throat, hence the amount of cavitation events goes up (Saharan et al., 2011). An excessive inlet pressure causes a drastic decrease in efficiency of removal. The cavitation number (C_v) has no unit. It expresses the state of cavitation in the inlet, it is the difference in pressure between the pressure at the outlet and the pressure at the inlet (Gogate, 2007). The following reaction expresses the cavitation number as follow $C_v = \frac{P_d - P_v}{0.5\rho_l V^2}$ with P_d (downstream pressure), P_v (solution vapour pressure). When the C_v value is less than 1 it shows evidence of vapour formation (Jain et al., 2014). At optimum conditions, the C_v value is between 0.15 and 0.25. in this range, excessive cavitation is avoided (Gogate et al., 2001). An increase in pressure at the inlet increases the velocity that decreases the cavitation number. The number of cavities generated increases with cavitation number (Jain et al., 2014).

2.3.5.3 Physicochemical proprieties of the liquid

Next to the HC pilot plant features, the physical and chemical properties of the sample plays a major role on the effectiveness of removal of POPs and initial bubble radius. Degradation in HC is temperature, vapour pressure, surface tension, catalyst and oxidising agent (FeSO_4 and H_2O_2), initial concentration of contaminant, viscosity and pH dependent. Temperature affects the rate at which the reaction between the OH radical and the organic pollutant occur. It affects the rate at which bubbles nucleate and collapse (Gogate, 2007). An increase in temperature causes a drop in the rate of cavitation. This induces a lower energy of collapse. In acidic medium, degradation is more favourable due to the favourable condition for the production of H_2O_2 which generates OH radicals. The oxidising potential of OH is higher in acidic conditions. In the same acidic condition, the decomposition of water is favourable to produce OH radicals (Tao et al., 2016). Higher value of vapour pressure increases the amount of cavities generated,

however, this increase in vapour pressure causes contaminant to move into the bubble reducing collapses. Some additives such as UV (FeSO_4) and H_2O_2 can be used to improve the production of OH radicals in hydrodynamic cavitation. However, excessive addition of catalyst and H_2O_2 reduce the potential of the OH radical, thus lowering the rate degradation of pollutants (Gagol et al., 2018). When the forces maintaining the liquid continuum are overcome, cavitation occurs. The higher the viscosity the lower the cavitation effect. An increase in viscosity results in an increase in energy and critical pressure needed for the formation of bubbles. Liquid with a high surface tension has the ability to achieve a high cavitation efficiency, the higher the need for the generation of bubbles, the higher the pressure needed to produce small bubble radius, thus a high collapse rate of cavities. This making the process very efficient. Surface tension affects the stability of the bubble, and the higher the surface tension, the more energy (pressure) is required to induce cavitation (Kumar et al., 2018). A rise in the concentration of the contaminant is expected to increase the extent of degradation as per thermodynamics law. However, it is observed in the case of degradation that a rise in the initial concentration of the contaminant causes a decrease in efficiency of the HC pilot plant (removal of contaminants). In fact, this is due to lower quantity of hydroxide radical to oxidise the pollutants (Chakinala et al., 2008).

The removal of organic material from solvent is very effective when the process goes through the generation of an intermediate radical with high oxidising or reducing potential. Trojanowicz reported this as the basis of AOPs techniques (Trojanowicz, 2020b). The removal of Orange II is known to include the presence of OH radical as an intermediate which in turn favours oxidation. Orange II is a salt and dissociate easily compared to PFOA. It forms intermediate that favors oxidation necessary for advance oxidation. The perfluorooctanoic acid is a strong acid that stabilises by induction due to the presence of many halogens (fluorine) which are electron withdrawing group. Its chemistry does not lead to the formation of such intermediate which favour oxidation. The interstate technology regulatory council confirmed that stability of PFOA by stating that PFOA are final products of the decomposition of perfluorooctane sulfonyl (ITRC, 2018).

It was reported that low temperature increases the decolouration of dyes (Gogate & Bhosale, 2013). The optimum temperature for the degradation of 2,4 dinitrophenol was found to be 35°C (Panda & Manickam, 2019), Tao and al. (2016) his co-worker reported arise in the extent of degradation of imidacloprid from $0.79 \times 10^{-3} \text{min}^{-1}$ to $1.27 \times 10^{-3} \text{min}^{-1}$ with a reduction in

the initial concentration from 60 ppm to 20 ppm using hydrodynamic cavitation (Patil et al., 2014; Badmus et al., 2020).

The extent of degradation in rhodamine B was found to be much higher employing swirling jet induced cavitation with addition of H₂O₂ than when using hydrodynamic cavitation only. The degradation extent of red K-2BP was reported to increase by ten times from $1.31 \times 10^{-3} \text{min}^{-1}$ to $1.25 \times 10^{-2} \text{min}^{-1}$ employing swirling jet induced cavitation with addition of 300 mg/L H₂O₂. A higher concentration of 300 mg/L H₂O₂ resulted in no significant increase (Wang et al.). The degradation of Red 88 and reactive Red 120 dyes was found to be 100% colour and 60% TOC removal using hydrodynamic cavitation and 60% colour and 28% TOC removal using hydrodynamic cavitation with H₂O₂ within 3 hours.

It was revealed that the combination of HC with Fenton reagent causes an increase of rate constant and removal of pollutants. This can be caused by the high production of OH radicals from decomposition of H₂O₂ in the presence of high amount of Fe²⁺ (Tao et al., 2016). The pressure of 3 bar at the inlet was reported to be the optimum pressure for the removal of diclofenac sodium using hydrodynamic cavitation (Bagal & Gogate, 2013).

The rise in the degradation caused by the addition of Fenton's reagent can be due to extended production of hydroxyl radicals caused by the conversion of Fe²⁺ to Fe³⁺ and successive reformation of ferrous ions under cavitating conditions. The added hydrogen peroxide is initially employed for the Fenton's process and a negligible amount gets directly converted to hydroxyl radicals. The extra hydrogen peroxide, along with the hydrogen peroxide produced as a result of hydrodynamic cavitation causes the continual generation of the oxidizing species (Patil et al., 2014).

It has been reported that the rate of degradation attained employing a slit venturi is higher than that achieved using orifices. At optimised value of operating variables 23.85% degradation of imidacloprid was reached by using orifice plate however under the same values of operating variables 27.93% degradation of imidacloprid was obtained in the case of the slit venturi (Patil et al., 2014). About 92% decolourisation Red 88 dye of Acid and 35% lowering in TOC was achieved at pH 2.0 using HC (Saharan et al., 2012). It was observed that the degradation yields of methyl orange rose with a reduction of the pH of the solution and a decolouration of the methyl orange of 73% was attained at pH 2 after 60 minutes (Innocenzi et al., 2018).

2.4 Process evaluation

2.4.1 UV-Vis spectrophotometry

UV-Vis spectrophotometry was employed to evaluate the extent of decolouration of dyes and PFOAs. It assessed the extent of removal of dye and PFOA by measuring the amount of UV light absorbed by the effluent's sample from the HC pilot plant. The instrument could be used for both qualitative and quantitative analysis, but in this work, quantitative analysis was more relevant. The UV technique is achieved on organic compound with unsaturation as observed in some group of organic molecules with double, triple bonds or resonance. It was thus used to identify dye as it has some unsaturation on its structure or chromophores. The UV technique can help determine the absorption intensity of a given organic compounds at a given wavelength. Beer-Lambert law to relate UV absorbance to the concentration of the solution linearly to make this analysis (Behera et al., 2012; Badmus et al., 2016; Peralta et al., 2014).

2.4.2 Material balance

The material balance is an estimation method used to evaluate over a process the law of conservation of mass which state that mass cannot be created or destroyed, the total mass is always conserved. The material balance determines the quantities entering and leaving the system, the quantities generated, consumed and the quantities accumulated within the system (Material, 1889). The material balance is a useful application for the evaluation of plant performance and troubleshooting and can be applied to examine operation in opposition to or close up to the design, to increase the frequently limited data obtainable from the plant instrument, to examine apparatus calibrations and to find causes of material loss (Sinnott, 2005).

2.4.3 Kinetic study: rate of reaction

Chemical kinetics is known as the study of the rates and mechanisms of chemicals reactions. The rate of reaction ($-r_A$) shows the speed at which a number of moles of one chemical components reacts to produce another chemical components. The kinetic study covered by Kumar on the treatment of ternary dye by HC has confirmed the data reported in the work covered by Badmus and Dular (Wang et al) that the removal of POPs obeys the pseudo first

order law on the same subject and worked out a way upon which most authors worked out the first order calculation (Dular et al., 2016; Badmus et al., 2020).

2.4.4 Energy balance and energy efficiency of the HC pilot plant

Energy balance expresses the concept of energy conservation. Energy can change from one form to another (for instance, potential energy can change to internal energy; internal energy stored in bonds can change into kinetic energy) but it cannot be created or destroyed. The energy balance is used to calculate the energy requirement of a process or to show the pattern of energy usage in an existing plant and suggest ways of improving efficiency (Sinnott, 2005). The energy balance is fundamental for illustrating the major cost and standard of process situation. (Material, 1899).

The **energy efficiency** of the HC reactor can be calculated by using the actual energy obtained from the power dissipated in the system. This energy was derived from energy balance calculations and checked against the overall energy supplied to the system in form of electrical power. Gogate, (2001) and Thanekar et al., (2021) linked the energy efficiency of the HC pilot plant found using a calorimetry study with the actual power dissipated in the system given by $P \text{ (Watt)} = mC_p \frac{dT}{dt}$ over supplied electrical power. With m , the mass of fluid in the system in Kg. With C_p , the heat capacity and in J/Kg °C and dT/dt , the change of temperature over time (Gogate et al., 2001), (Thanekar & Gogate, 2018).

The energy efficiency can also be determined on the basis of the cavitation yield. This last is known as the amount of pollutant removed per unit energy consumed which is given by: $\text{Cavitation yield} \left(\frac{mg}{L} \right) = \frac{\text{Amount of pollutant degraded}}{(P_m t)V}$ with P_m , t and V being the pump power, the time of operation and the volume of pollutant solution respectively (Panda & Manickam, 2019).

2.4.5 Production cost

Any engineering project requires a good account of the resources used. When the prices of resources are known they are derived from the bills, and when they are unknown, an estimation is necessary. Cost estimation is a forecasting method used to determine the costs of resources

required by the scope of a project. These costs can be classified as capital investment and total production costs (Karl Kolmetz, 2014).

Total capital investment involves the total amount of money needed for the payment of land, design, equipment, installation, buildings and for taking the facility into operation (Saravacos & Maroulis, 2007). The total capital investment is given by the overall fixed capital investment and working capital (Sinnott, 2005).

Fixed capital stands for the cost paid to the contractors for the construction of a plant. It involves the expenses on design, engineering, construction, supervision, equipment and their installation, all instrumentation and control systems, the cost of building and structures, additional facilities such as utilities, civil engineering work and land (Sinnott, 2005). On the other hand, working capital is the cost involved in the start-up and operation of the plant before process profit begin (Karl Kolmetz, 2014). Working capital represent 5 to 30% of the fixed capital (Sinnott, 2005).

2.4.5.1 Estimation of capital investment cost

Capital investment costs can be estimated using the rapid capital cost estimating method or the factorial method of estimating cost (Sinnott, 2005).

2.4.5.2 Rapid capital cost estimating method

This method generates the capital cost obtained using the cost of previous similar projects (historical costs) and it is given by the equation:

$$C_2 = C_1 \left(\frac{S_2}{S_1} \right)^n$$

C_1 and C_2 representing capital cost of the project with capacity S_1 and S_2 respectively, n representing the value of the index which is generally established as 0.6 defined as six-tenths rule.

The capital cost is obtained using the step counting method which includes some processing steps in the general processes, some factors such as: operating pressure, temperature, material of construction and a yield for the assessment of the complexity of the process. The capital cost (C) for a plant handling mostly liquid or solid phase processes with capacities under

60,000 tonnes per year is given by $C = 130,000 N(\frac{Q}{S})^{0.30}$ or $C = 150 N(\frac{Q}{S})^{0.675}$, and for processes with capacities above 60,000 tonne per year, and $C = 8000 N(\frac{Q}{S})^{0.615}$ for gas phase processes, with N, Q and S representing the plant capacity (tonne per year), number of functional units, and reactor conversion respectively. The conversion of the reaction is calculated as:

$$S = \frac{\text{mass of desired product}}{\text{mass reactor input}}$$

2.4.5.3 Factorial method

Factorial method makes provision for technique of cost estimation; it provides that capital cost is estimated using two parameters: the estimate of the purchase costs on major equipment components and the second is the cost estimation of the factors affecting equipment cost. The Factorial method is made up of Lang factor method and of detail factorial estimate. Lang factor provides that the fixed capital cost is evaluated as a function of the total equipment purchase, and it is expressed in the equation: $C_f = f_L \cdot C_e$ with C_f, C_e in which f_L representing respectively the fixed capital cost, the total delivered cost of all the major equipment items and the Lang factor which depends on the type of processes. For solids processing plants, the constant processing value is $f_L = 3.1$; for fluids solids plants, $f_L = 3.6$; for fluids processing plants, $f_L = 4.7$ (Sinnott, 2005).

The detail factorial estimate method includes the cost factors estimation for all parameters. However, in Lang factor method, factors of solid, liquid and gas are compounded in one term. The direct and the indirect cost items involved in the construction of a plant added to the cost of equipment are listed in the table below. The contribution of each item to the direct cost and to the total cost is found by multiplying the total purchased equipment by a convenient factor which are derived from historical cost data for similar processes. The indirect costs can be estimated as a function of the direct costs. The fixed capital investment is given by the sum of direct and indirect costs (Sinnott, 2005).

Table 2.1 Factors of direct and indirect cost items used for the estimation of the fixed capital cost (Sinnott, 2005)

Item	Process type			
	Fluids	Fluids-solids	Solids	
1. Major equipment, total purchase cost	PCE	PCE	PCE	
f_1 Equipment erection	0.40	0.45	0.50	
f_2 Piping	0.70	0.45	0.20	
f_3 Instrumentation	0.20	0.15	0.10	
f_4 Electrical	0.10	0.10	0.10	
f_5 Buildings, process	0.15	0.10	0.05	
f_6 Utilities	0.50	0.45	0.25	
f_7 Storage	0.15	0.20	0.25	
f_8 Site development	0.05	0.05	0.05	
f_9 Ancillary buildings	0.15	0.20	0.30	
2. Total physical plant cost (PPC)				
PPC = PCE (1 + f_1 + ... + f_9)				
	= PCE ×	3.40	3.15	2.80
f_{10} Design and Engineering		0.30	0.25	0.20
f_{11} Contractor's fees		0.05	0.05	0.05
f_{12} Contingency		0.10	0.10	0.10
Fixed capital = PPC (1 + f_{10} + f_{11} + f_{12})				
	= PPC ×	1.45	1.40	1.35

PPC and PCE represent the physical plant cost and the purchase cost equipment respectively. f_1 to f_9 represent the different factors for the direct costs items and f_{10} to f_{12} represent the factors for the indirect costs items.

2.4.5.4 Total production cost and operating cost

Total production costs are costs including the operations of the plant and the sale of products. Total production cost includes operation costs and general expenses (Karl Kolmetz, 2014). Operation costs are also called manufacturing costs. It is the cost involved in the normal operation of a component or a facility involving labour, material, utilities and other sale costs. Operating costs are classified as direct production costs, fixed charges and plant overhead costs. Direct cost are costs are associated with a specific product or process (Karl Kolmetz, 2014). Direct costs include variable and semi-variable costs. Variable costs are cost which change with direct proportion to the production rate. Utilities, supply, laboratory charges are examples of these costs. Semi-variables costs are costs which do not change directly with the

production rate. Maintenance, supervision, labour and payroll charges are examples of these costs. Fixed charges are costs which do not change as the production costs vary. Depreciation, taxes, etc. are examples of these costs. Plant overhead costs are plant indirect costs such as security, fire protection, roads, yards, and docks (Saravacos & Maroulis, 2007).

The general expenses are general costs additional to operating cost. The general expenses include administrative costs, distribution, marketing cost, research and development cost as well as financial cost (Karl Kolmetz, 2014).

2.5 Chapter summary

The literature covered the removal of persistent contaminant from wastewater. It highlighted the various methods known to date including the one showing limitation in the removal of contaminants. The choice of hydrodynamic cavitation among advanced oxidation techniques was considered helpful to the objectives of this study. In fact, it helped optimise the process of removal of dye as contaminant from a simulated industrial wastewater by providing evidence around the impact of time, catalyst, oxidising agent, the Fenton reagent, orifices of various sizes, the venturi and the combination of both cavitating devices. The optimised condition is a simple pathway for efficient removal of contaminants that would be applicable to the remediation of clean water scarcity concerns. The optimum conditions are to be used for the removal perfluorooctanoic acid in this study.

3. CHAPTER 3. RESEARCH DESIGN AND METHODOLOGY

Chapter 3 illustrates how the experiments were carried out, the material, the apparatus and the analytical methods employed.

3.1 Experimental outline

The experiments were conducted following the schematic below

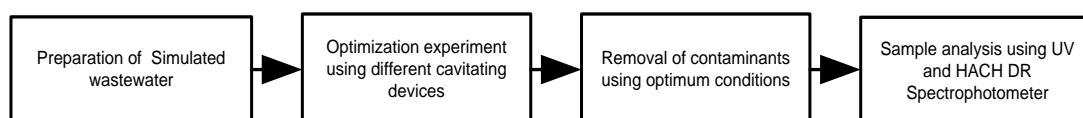


Figure 3.1 Schematic diagram of removal of POPs

3.1.1 Material

Table 3.1 Table of standards

Standards	Purity	Use	Supplier
Orange II sodium dye (C ₁₆ H ₁₁ N ₂ NaO ₄ S)	99%	To prepare simulated wastewater	Sigma- Aldrich
Sulphuric acid (H ₂ SO ₄)	98%	To reduce pH	Sigma- Aldrich
Hydrogen peroxide (H ₂ O ₂)	30%	To enhance OH radicals and prepare Fenton reagent	Sigma- Aldrich
Ferrous sulphate (FeSO ₄ .7H ₂ O)	99%	As a catalyst and added to hydrogen peroxide to form Fenton reagent to enhance OH radicals production	Sigma- Aldrich
Perfluorooctanoic acid	96 %	To prepare simulated wastewater	Sigma- Aldrich
Distilled water		To prepare 20 ppm orange II dye solution	UWC Chemistry laboratory

3.1.2 Apparatus

Table 3.2 The table of instruments used

Instruments	Utilities
Scale	To weigh chemicals
pH meter	To measure the pH
HC pilot plant	To generate OH radicals
UV spectrophotometer	To determine the absorbance from which the degraded concentration is found
HACH DR/2010	To measure the COD

3.1.3 Experimental Set up

The figures below depict a schematic representation of HC pilot plant and the constriction used in the work. The system mainly consists of a circular-loop made up of a holding tank of 80 L in volume, a centrifugal pump (2650 rpm, 2.2 KW, 400 V), a cavitation chamber involving venturi or orifice, control valves to regulate the flow-rate through the constriction, pressure and temperature gauge devices.

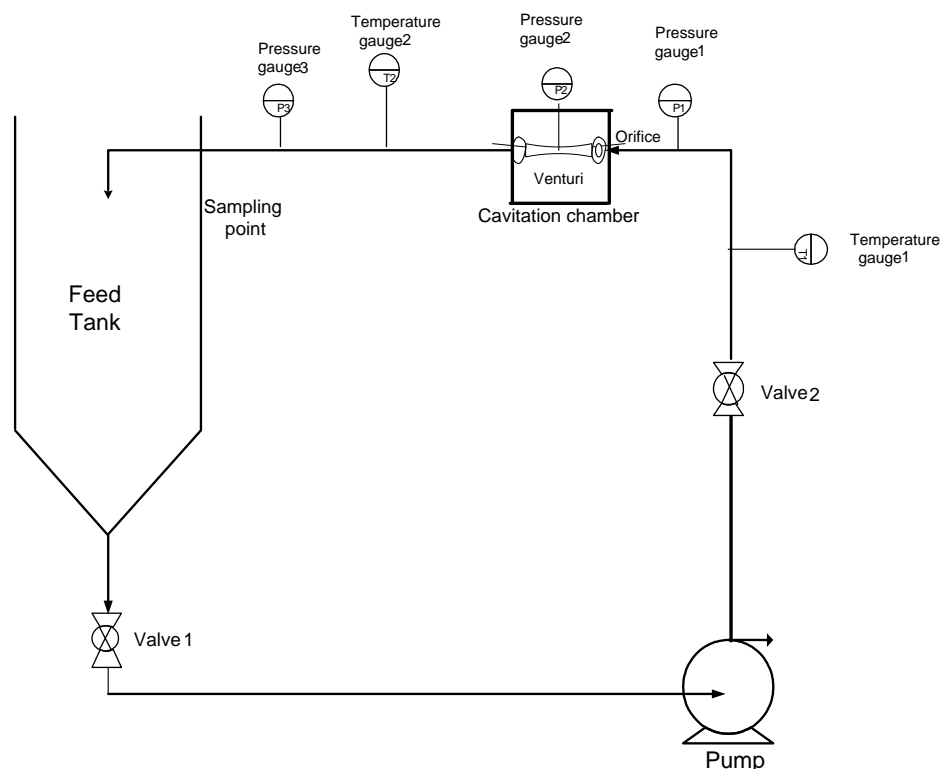


Figure 3.2 Hydrodynamic cavitation flow diagram schematic representation



Figure 3.3 Actual photograph of hydrodynamic cavitation pilot plant

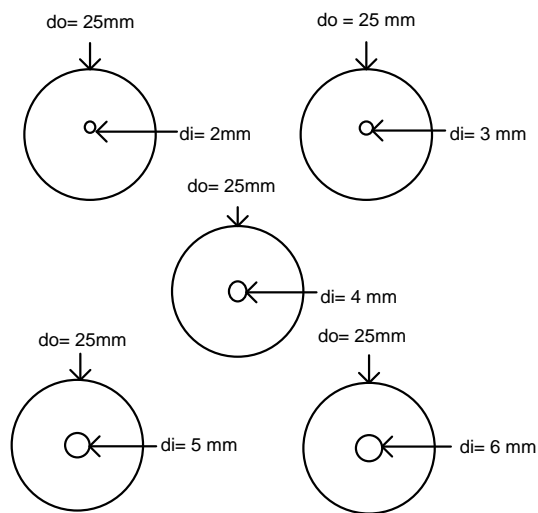


Figure 3.4 Schematic representation of orifices cavitating device with 3mm thickness each



Figure 3.5 Actual photograph of orifices cavitating device

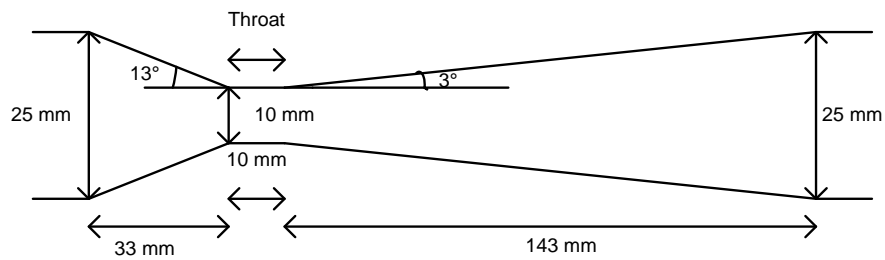


Figure 3.6 Schematic representation of the venturi cavitating device and its actual picture

3.1.4 Experimental procedure

The orange II dye solution of concentration 20 ppm was prepared using distilled water. Constant total reaction volume was kept at 10 L which solution was brought to pH 2 using sulphuric acid and placed in the feed tank. Treatment time was varied between 60 and 10 minutes and sampling interval time as 10 and 2 min respectively. The inlet pressure was

adjusted to 300 KPa as reported in a similar investigation (Badmus et al., 2020). The flow-rate of the sample was optimised by varying cavitating devices (orifices 2, 3, 4, 5 and 6mm) initially, then using a 10 mm throat for the circular venturi alone. The same experiment was repeated with the orifice using 100 mg of Iron (II) catalyst in the form of iron sulphate, first and then with 10 ml of an oxidising agent: hydrogen peroxide. The preceding experiment were conducted for 60 min time period with a 10 min sampling time. This experiment was finally repeated for 10min without iron as the catalyst nor the oxidising agent. It was this step which defined the optimum technique. The same procedure was used to prepare the PFOA samples but only using 2 mm orifice alone. The proceed from the removal on the HC pilot plant was analysed using for Chemical Oxygen Demand with the DR/2010 spectrophotometer.

All the experiments conducted in this work took place at pH 2 as it was observed previously that at acid pH of 2 the best removal of dyes was observed (Badmus et al., 2020).

Table 3.3 Experimental details for optimisation of Hydrodynamic cavitation

Fixed and varied parameters	First set
60 min experiment run, 10 min sampling time, 300 Kpa inlet pressure, 10L solution volume, 20 ppm orange II concentration	Orifice 2 mm hole (O2)
	Orifice 3 mm hole (O3)
	Orifice 4 mm hole (O4)
	Orifice 5 mm hole (O5)
	Orifice 6 mm hole (O6)
	Venturi 10 mm throat (V)
Fixed and varied parameters	Second set
60 min experiment run, 10 min sampling time, 300 Kpa inlet pressure, 10L solution volume, 20 ppm orange II concentration plus 100 mg of iron sulphate	Orifice 2 mm hole (O2)
	Orifice 3 mm hole (O3)
	Orifice 4 mm hole (O4)
	Orifice 5 mm hole (O5)
	Orifice 6 mm hole (O6)
Fixed and varied parameters	Third set
60 min experiment run, 10 min sampling time, 300 Kpa inlet pressure, 10L solution volume, 20 ppm orange II concentration plus 10 ml of hydrogen peroxide	Orifice 2 mm hole (O2)
	Orifice 3 mm hole (O3)
	Orifice 4 mm hole (O4)
	Orifice 5 mm hole (O5)

	Orifice 6 mm hole (O6)
--	------------------------

Fixed and varied parameters	Fourth set
60 min experiment run, 10 min sampling time, 300 KPa inlet pressure, 10L solution volume, 20 ppm orange II concentration plus 100 mg of iron sulphate and 10 ml of hydrogen peroxide	Orifice 2 mm hole (O2)
	Orifice 3 mm hole (O3)
	Orifice 4 mm hole (O4)
	Orifice 5 mm hole (O5)
	Orifice 6 mm hole (O6)

Fixed and varied parameters	Fifth set
10 min experiment run, 2 min sampling time, 300 KPa inlet pressure, 10L solution volume, 20 ppm orange II concentration	Orifice 2 mm hole (O2)
	Orifice 3 mm hole (O3)
	Orifice 4 mm hole (O4)
	Orifice 5 mm hole (O5)
	Orifice 6 mm hole (O6)
	Venturi 10 mm throat (V)

3.2 Instrumental analysis

The concentration of orange II in solution was analysed using UV-visible spectrophotometer. A 1 ml sample solution was taken, the absorbance measured at 483 nm and plotted on a calibration chart obtained by evaluating the absorbance of standard solution of orange II Versus its standard concentrations.

3.2.1 Material balance

Material balance is expressed by the following equation:

$$\text{Accumulation} \left(\frac{dm}{dt} \right) = \text{Input} (m_{in}) - \text{Output} (m_{out}) + \text{Generation} (G) - \text{Consumption} (G')$$

3.2.2 Kinetics studies

Kinetic study measures the rate at which a chemical reaction takes place. It can help monitor the rate of reaction at which one mole of a chemical component A undergoes a chemical reaction which turns it into a product P as suggested by the following reaction ($A \rightleftharpoons P$).

$$F_{Ao} - F_A + \int_0^V r_A dV = \frac{dN_A}{dt} \quad (1)$$

With F_{Ao} being the rate at which A flows into the system (moles/time)

F_A being the rate at which A flows out of the system (moles/ time)

$\int_0^V r_A dV$ being the rate at which A is being generated (moles/ time)

$\frac{dN_A}{dt}$ being the rate at which A accumulate in the system (moles/ time)

There is no inflow nor outflow of reactants for batch reactor involving small scale operation, nor products for the reaction taking place, thus $F_{Ao} = F_A = 0$,

The mole balance equation is given by : $\frac{dN_A}{dt} = \int_0^V r_A dV$

If there is no change in the rate of reaction throughout the reactor, the new reaction is given

by: $\frac{dN_A}{dt} = r_A dV \quad (1)$

For a constant volume batch reactor, $V = V_0$, thus equation (1) can be written in the form:

$$\frac{1}{V_0} \frac{dN_A}{dt} = r_A$$

$$\frac{d(N_A/V_0)}{dt} = r_A$$

$$\frac{dC_A}{dt} = r_A \quad (2)$$

The algebraic equation that relates the rate of reaction to concentration of component A is given by: $-r_A = kC_A^\alpha$

With k being the rate of reaction constant and α being the order of the reaction

Thus, equation (2) can be written as:

$$-\frac{dC_A}{dt} = kC_A^\alpha$$

The reaction order in a batch reactor can be determined by: differential, integral or nonlinear regression method.

In differential analysis, the reaction order is determined using the slope α obtained from sketching $\ln(-\frac{dC_A}{dt})$ versus $\ln C_A$. It is found by taking in consideration both sides of the equation ($\ln(-\frac{dC_A}{dt}) = \ln k + \alpha \ln C_A$) after finding $-\frac{dC_A}{dt}$ from the plot of $-\Delta C_A/\Delta t$ as a function of time, t .

Integral Method:

The reaction order is determined by guessing the reaction order and by integrating the differential equation ($-\frac{dC_A}{dt} = kC_A^\alpha$), which should be linear when plotted as a function of time.

A zero order reaction is expressed by, $\frac{dC_A}{dt} = -k$, integrating from C_A at time t to C_{A0} at time $t = 0$ give $C_A = -kt + C_{A0}$, the plot of C_A versus time should be linear with slope k .

If a reaction is first order, $-\frac{dC_A}{dt} = kC_A$, integrating from C_A at time t to C_{A0} at time $t = 0$ give $\ln \frac{C_{A0}}{C_A} = kt$, the plot of $\ln \frac{C_{A0}}{C_A}$ versus time should be linear with slope k .

If a reaction is second order, $-\frac{dC_A}{dt} = kC_A^2$, integrating from C_A at time t to C_{A0} at time $t = 0$ give $\frac{1}{C_A} = kt + \frac{1}{C_{A0}}$, the plot of $(\frac{1}{C_A})$ versus time should be linear with slope k .

In nonlinear regression: the reaction order is determined by using polymath regression after integration the differential rate equation resulting in $t = \frac{1}{k} [\frac{C_{A0}^{1-\alpha} - C_A^{1-\alpha}}{1-\alpha}]$ with $\alpha \neq 1$

C_A and C_{A0} represent respectively the concentration of A at time (t) and the initial concentration of A.

3.2.3 Energy efficiency

The general equation of energy balance is expressed as

Accumulation of energy in a system = Input of energy into the system – output of energy from the system + energy generated within the system – energy consumption within the system

In HC reactor, the input of energy into the system is electrical energy which is converted to mechanical energy through liquid flow and pressure which is converted to heat energy resulting in a rise in temperature. The pressure due to collapsing bubbles produces cavities which induce oxidation reactions. Thus, the total energy of a system is constituted by kinetic, potential

and internal energy. Kinetic energy (E_k) is related with flow of the system, it is given by $E_k = \frac{1}{2}mv^2$, with m and v representing respectively mass and velocity; Potential energy is result from the position of a system in a gravitational field, it is given by $E_p = mgz$ with m, g and z representing respectively the mass, the gravitational acceleration and the elevation in the gravitational field; Internal energy (U) is due to all atomic, subatomic and molecular movement and reactions. These energies can be carried into or out of the system by flow of mass (\dot{m}) through process streams, by flow of heat (\dot{Q}) or by performance of work (\dot{W}) that transport the diverse type of energy with them.

By expressing all terms as rates, equation 1 becomes

$$\frac{dE_k}{dt} + \frac{dE_p}{dt} + \frac{dU}{dt} = \sum_{input\ streams} \dot{m}_{in} \left(\hat{U}_{in} + \frac{v_{in}^2}{2} + gz_{in} \right) - \sum_{output\ streams} \dot{m}_{out} \left(\hat{U}_{out} + \frac{v_{out}^2}{2} + gz_{out} \right) + \dot{Q} - \dot{W} \quad (2)$$

The total rate of work (\dot{W}) is given by $\dot{W} = \dot{W}_s + \dot{W}_{ft}$ with \dot{W}_s and \dot{W}_{ft} representing respectively the shaft and flow work. The shaft work is associated with the force exerted by moving parts of a system's boundary across which there is no mass flow. In HC reactor, the shaft work is provided by the pump. The flow work is related to the force exerted by the flowing particles at the input and output streams. It is given by $\dot{W}_{ft} = -P\dot{V}$ with P and \dot{V} representing respectively the pressure and the volumetric flow rate.

By writing the total rate of work by its formula, equation (2) becomes:

$$\frac{dE_k}{dt} + \frac{dE_p}{dt} + \frac{dU}{dt} = \sum_{input\ streams} \dot{m}_{in} \left(\hat{U}_{in} + P_{in}\dot{V}_{in} + \frac{v_{in}^2}{2} + gz_{in} \right) - \sum_{output\ streams} \dot{m}_{out} \left(\hat{U}_{out} + P_{out}\dot{V}_{out} + \frac{v_{out}^2}{2} + gz_{out} \right) + \dot{Q} - \dot{W}_s \quad (3)$$

By inserting the enthalpy which is given by $\hat{H} = \hat{U} + P\dot{V}$, equation (3) become :

$$\frac{dE_k}{dt} + \frac{dE_p}{dt} + \frac{dU}{dt} = \sum_{input\ streams} \dot{m}_{in} \left(\hat{H}_{in} + \frac{v_{in}^2}{2} + gz_{in} \right) - \sum_{output\ streams} \dot{m}_{out} \left(\hat{H}_{out} + \frac{v_{out}^2}{2} + gz_{out} \right) + \dot{Q} - \dot{W}_s \quad (4)$$

Also, considering $\hat{H} = C_p(T - T_{ref})$, and $\hat{H} = \hat{U} + P\dot{V}$, equation (3) turns into :

$$\frac{dE_k}{dt} + \frac{dE_p}{dt} + \frac{dU}{dt} = \sum_{input\ streams} \dot{m}_{in} \left(C_{p_{in}}(T_{in} - T_{ref}) + \frac{v_{in}^2}{2} + gz_{in} \right) - \sum_{output\ streams} \dot{m}_{out} \left(C_{p_{out}}(T_{out} - T_{ref}) + \frac{v_{out}^2}{2} + gz_{out} \right) + \dot{Q} - \dot{W}_s \quad (5)$$

The efficiency expresses the amount of energy needed to complete the full process.

$$\text{Energy efficiency (\%)} = \frac{\text{Actual power dissipated in the system}}{\text{Supplied electric power}} \times 100$$

The energy efficiency can also be determined based on the cavitation yield which is given

$$\text{by: Cavitation yield } \left(\frac{\text{mg}}{\text{L}} \right) = \frac{\text{Amount of pollutant degraded}}{(P_m t) V}$$

3.3 Analytical methods

The following analytical methods were used in this experiment:

3.3.1 UV analysis

UV analysis data output were obtained using the CDC UV VIS 920 spectrophotometer and plotted on a Cartesian plan so that the independent variables x-axis (concentrations) and the dependant variable on the y axis, absorbance were connected according to the following law. The UV spectrophotometer was used to measure the absorbance of orange II dye solution collected after running experiments. For the analysis of sample of orange II dye, the peak of the wavelength was set at 483 nm. There was linearity between the absorbance and the concentration according to Beer Lambert and Bouguer.

$$A = \text{Log}T = \epsilon lc$$



Figure 3.7 UV Vis-spectrophotometer instrument

3.3.2 Chemical Oxygen Demand

The PFOA sample was prepared according to the procedure in section 3.1.4 and was analysed using the HACH DR/2010 spectrophotometer at 620nm. Chemical oxygen demand (COD) is an analytical method assessing the level of pollutant that are dissolved in waste sample. It is also used as a mean to assess the amount of dissolved organic material after removal from wastewater. Lo et al. (2018) referred to it as the number of substances needed to oxidise the organic sample under investigation. This technique is used to monitor the removal of perfluorooctanoic acid from the sample under the optimised condition of removal of dyes. This technique is spectral and it has been reported to be very accurate at assessing the amount of organic material dissolved (Li et al., 2018).

The method followed to analyse sample using COD is documented. It involved combining a mixture of 2.5 mL of distilled water, 1.5 mL of potassium dichromate and 3.5 mL of sulphuric acid as catalyst in a pre-dried vial. Samples from the oven were placed in a COD reactor maintained at 150 degrees for two hours. Samples were run using an Hach DR/2010 spectrophotometer at an absorbance of 620 nm. This absorbance instrument provided the final result.



Figure 3.8 HACH DR/2010 machine (HACH, 2010)

3.3.3 pH-meter

A pH-meter is an instrument which determines the acidity or alkalinity by measuring the concentration of hydrogen ion through a glass electrode immersed in a solution. In this study, a pH meter was used to monitor the pH of orange II dye solution.

3.3.4 Data analysis

The calibration curve was plotted using concentration of 0, 5, 10, 20 ppm of orange II dye solution versus absorbance resulting from these concentrations in order to find the slope of the curve which is used to calculate the degradation concentration of contaminants.

Table 3.4 Absorbance measurement

Orange II dye concentration (ppm)	Absorbance
0	0
5	0,3749
10	0,6935
20	1,2668

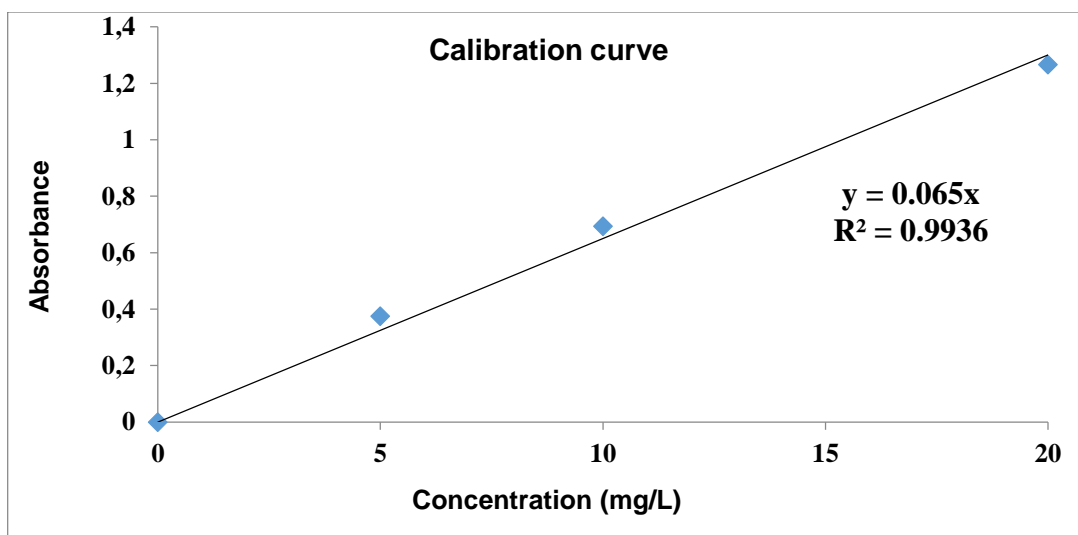


Figure 3.9 UV-Vis Calibration curve for orange II dye

Table 3.5 Chemical oxidation demand measurement

PFOA concentration (ppm)	Chemical oxidation measurement (mg/L)
0	0
2	33
4	6
6	4
8	6
10	23

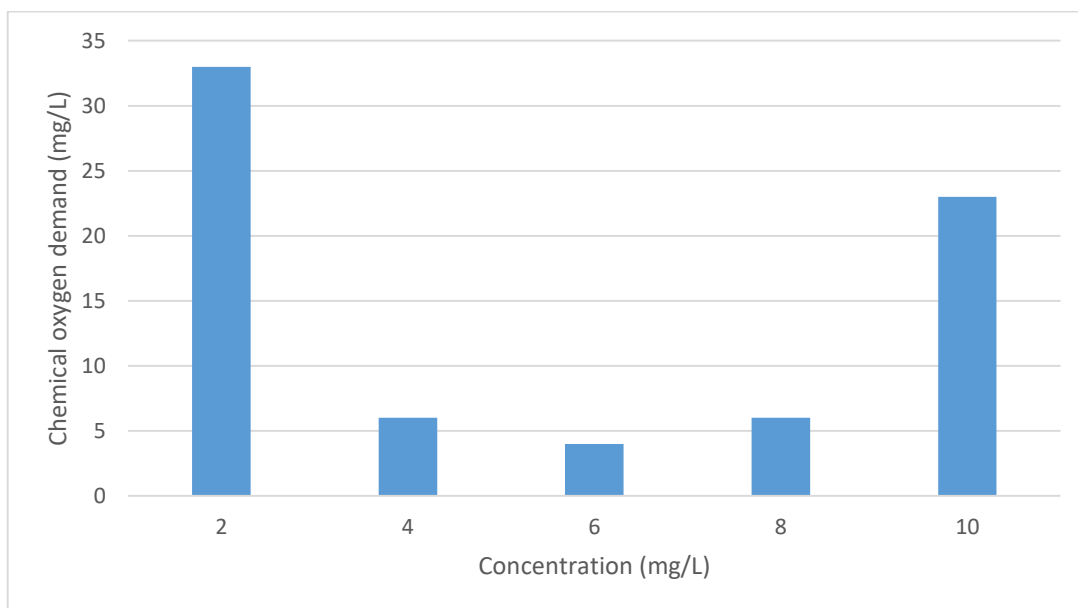


Figure 3.10 PFOA data measurement

3.4 Summary

This chapter described the chemical, the apparatus, the experimental procedure for the optimization of Hydrodynamic cavitation HC pilot plant and the analysis protocol used with the UV Vis and DR/2010 spectrophotometer to determine the percentage removal of dyes and /or chemical oxygen demand removal of PFOA.

4. CHAPTER 4. RESULTS AND DISCUSSION

4.1 Optimization of hydrodynamic cavitation on dye removal

This chapter provides and discusses the results of the optimization of HC pilot plant toward the removal of the selected contaminant dye in wastewater. It also provides the results of the removal of the perfluorooctanoic acid contaminant from wastewater at the optimum conditions as summarised in Appendix A.

4.1.1 Effect of different cavitating devices on dye decolouration

Wastewater containing Orange II dye was allowed to run for 60 minutes on the HC pilot plant using the orifice 2 (O2), 3 (O3), 4 (O4), 5 (O5) and 6 (O6) mm separately from the venturi with the sampling taking place respectively at 10, 20, 30, 40, 50 and 60 min for specific orifices. The venturi data were applied and compared to orifice as depicted in Figure 4.1.

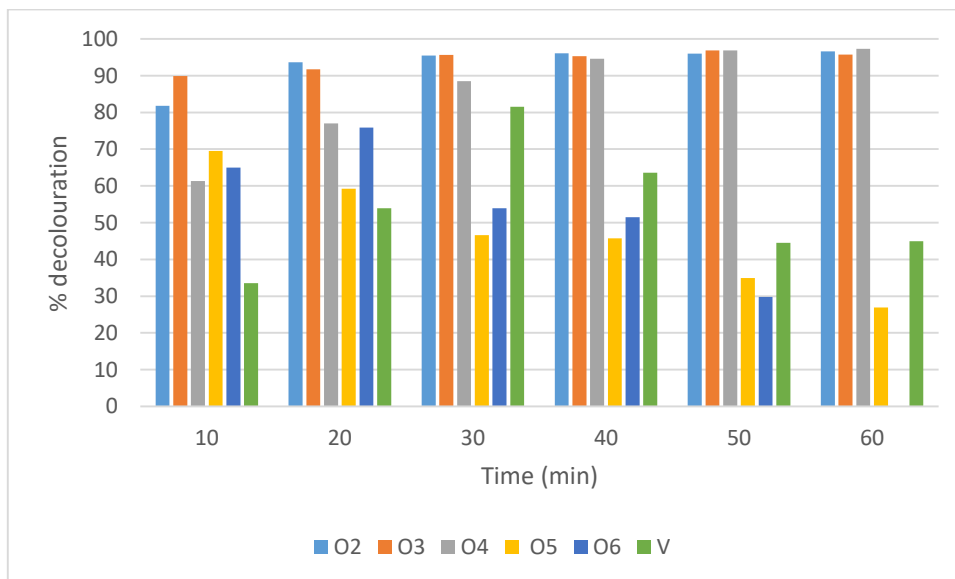


Figure 4.1 Effect of different cavitating devices on dye decolouration in the HC pilot plant (Fixed parameters: Orange II concentration 20 ppm, 10 L solution volume, solution pH 2, 60 min experiment, 10 min sampling interval, 300 KPa inlet pressure, 22°C starting temperature)

The decolouration of orange II dye in Figure 4.1 showed a rapid increase in the process of decolouration using the orifices between 0 and 10 min for orifice 2 (O2), 3 (O3) and 4 (O4). The venturi showed improvement in decolouration from 10 to 30 min and then decreased in effectiveness from 30 min to 60 minutes, showing an optimum time at around 30 minutes..

Orifice O5 had a good decolouration only between 0 and 40 minutes while a decline in its effectiveness was observed from 10 to 60 min. Orifice O6 was only effective from 10 to 20 min and then decrease. These observations made the orifice O2, O3 and O4 to give the highest decolouration efficiency. As the graph is observed across the 60 min experimental period, it was observed that O2 had a nearly steady state of decolouration, this was not the case with orifices O4 and O5 where in the late a decrease was observed as the experiment was observed in 60 minutes and the former showed an increase then a decrease. The reason for this observation lied in the size of the orifice. When the orifice size was larger, the removal wasn't significant this is the case of the venture which had a throat with size 10 mm and O4 and O5. A large orifice size or constriction results in lower fluid flow rate, thus less pressure build up; in these conditions, literature report that an excessive pressure recovery would result in the formation of larger cavities which do not collapse, hence reduced the number of hydroxyl radical and the percentage decolouration of orange II dye at the same time. This showed that decolouration can be achieved under specific condition of pressure and temperature (Saharan et al., 2012). Gagol et al. (2018), and Gogate (2007) suggests that a rise in temperature reduces the rate of decolouration (Gagol et al., 2018; Gogate, 2007).

4.1.2 The effect of orifice size on the presence of Iron sulphate and hydrogen peroxide

4.1.2.1 Removal of dye using 100 mg of Iron sulphate within 60 min

The introduction of iron (II) to the procedure described in section 4.1.1 applying only to orifices gave rise to the result in Figure 4.2. The venturi was not providing good decolouration due to the size of their throat as discussed in section 4.1.1 being large and the catalyst not showing any improvement to it. Therefore, the parameters remained 20 ppm concentration for Orange II dye, a 10 L volume, 100 mg Iron sulphate, pH 2 solution, 60 min experiment, sampling interval of 10 min, 300 KPa of inlet pressure, 22°C starting temperature.

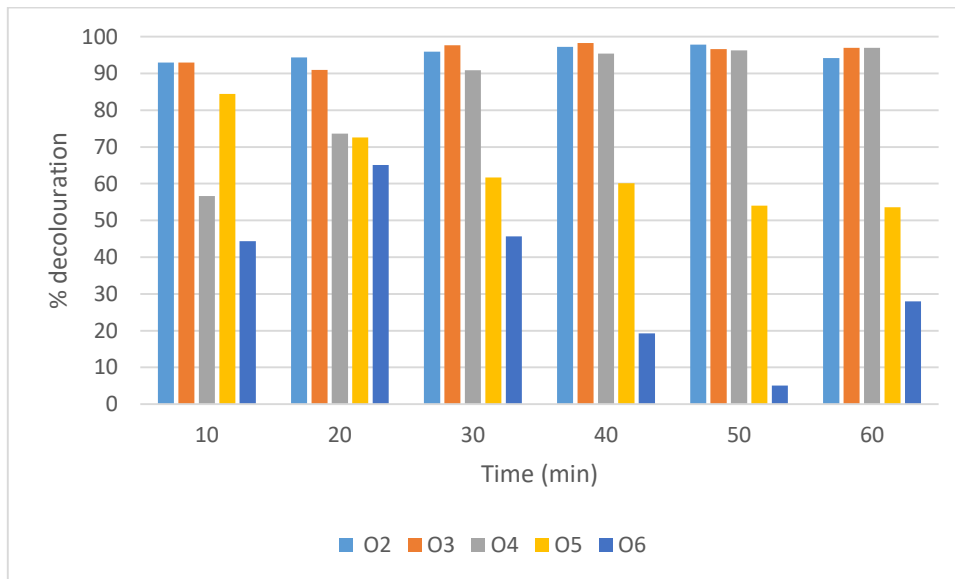


Figure 4.2 Effect of orifice size and catalyst (iron sulphate) on dye decolouration show O2, O3 and O4 had good decolouration efficiency.

The decolourisation process of orange II in Figure 4.2 expressed the impact of iron sulphate addition on dye decolouration. The use of a catalyst in the process of dye decolouration improved the process. As observed before, the initial increase of dye decolouration was greater in the region between 0 and 10 min. In fact, when comparing Figure 4.1 and Figure 4.2, orifice 2 showed an increase from 82 to 93% after 10 min when iron sulphate was added, Orifice 3 decolouration efficiency increased from 90 to 93% and orifice 4 showed an increase from 70 to 84%. Orifice 5 and 6 caused the efficiency of the system to decrease after 10 min in the presence of the catalyst. In fact, orifice 6 efficiency decreased from 85 to 75% and the orifice 5 decreased from 65 to 44%. This decrease can be attributed to an excessive amount of iron in the dye solution causing a depletion of hydroxyl radicals resulting in a lower oxidation of dye (Chakinala et al., 2008).

4.1.2.2 Removal of dye using 10 mL hydrogen peroxide (oxidising agent) within 60 min

The effect of an oxidizing agent to the same process of decolouration as in section 4.1.1 was studied here for various orifices cited before. Parameters such as pressure, temperature and feedstock volume, pH, initial temperature were kept the same as in the previous scenario.

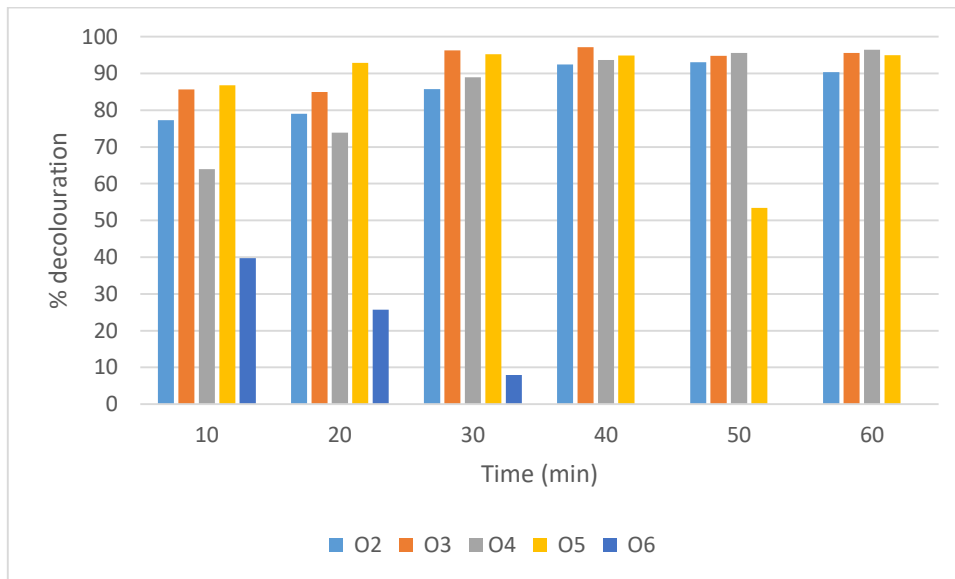


Figure 4.3 Effect of orifice size in the presence of hydrogen peroxide on dye decolouration (Fixed parameters: Orange II concentration 20 ppm, solution volume 10 L, hydrogen peroxide 10 mL, solution pH 2, experiment run for 60 min, sampling interval of 10 min, inlet pressure of 300 KPa, starting temperature 22°C)

The process presented in Figure 4.3 was studying decolouration as a result of addition of 10 ppm of hydrogen peroxide, an oxidising agent. The process proved to be very efficient for all the orifices used except for the 6 mm one where a drastic decrease in decolouration was noticeable from the same bar graph. In fact, decolouration was rapid within 10 min for all orifices. When comparing the decolouration between Figure 4.1 and Figure 4.3 at 10 min, orifice 2 increased from 70 to 87%. The percentage decolouration of orange II dye using orifice 2, 3, 4 and 6 mm decreased when peroxide was added. For instance, at 10 min the percentage decolouration of orange II dye was slightly reduced for orifice 2, 3, 4 and 5 respectively from 82% to 77%, from 90% to 86%, from 83% to 82% and from 65% to 40%. After 10 min, the decolouration continued on with a smaller gradient so that decolouration increased slightly. This decrease can be assigned to an excessive amount of hydrogen peroxide used to generate the hydroxyl radical beyond a specific concentration of RO_4 its POP. In fact, Gore et al. (2014) observed the same phenomena for a high concentration in hydrogen peroxide exceeding passed a specific molar concentration of the species in solution $H_2O_2:RO_4$. An excess amount of hydrogen peroxide would cause the produced HO to be scavenged as a result of scavenging of the produced OH radicals by H_2O_2 (Gore et al., 2014). Although the percentage decolouration was decreased, the removal trends indicated an efficient process (Saharan et al., 2011). The orifice 6 had poor removal due to poor pressure drop as motivated in section 4.1.1.

4.1.2.3 Removal of Orange II using (Fenton reagents) within 60 min

The use of 100 mg of iron sulphate mixed with 10 mL hydrogen peroxide to form a solution known as the Fenton reagent was applied to the decolouration processes in section 4.1.1 for orifice. This gave rise to Figure 4.4 below. The physical parameters such as temperature, pressure, and feedstock volume, pH, initial temperature remained the same as in the initial experiment. No venturi data were collected due to the large size of the throat.

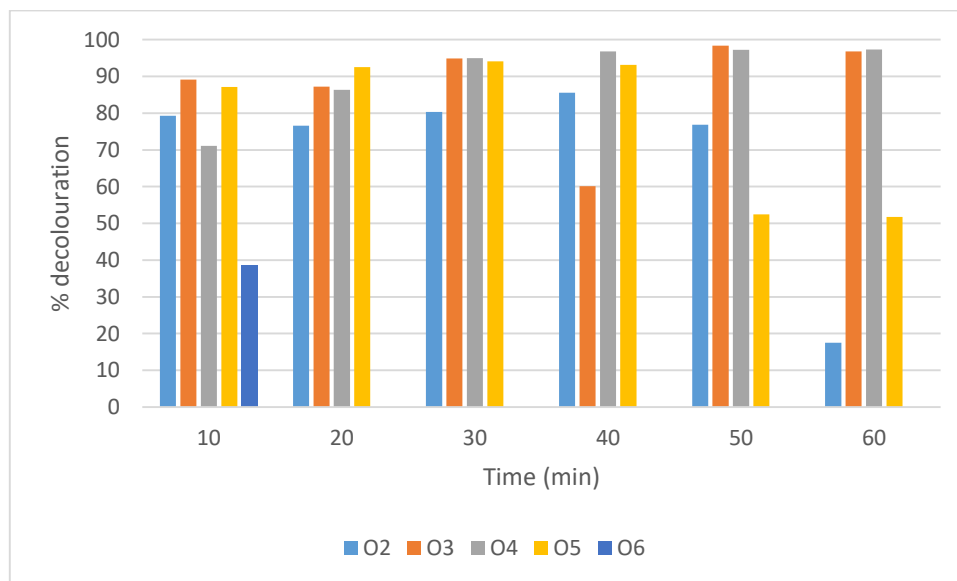


Figure 4.4 Effect of decolouration using orifice size 2, 3, 4, 5 and 6 in the presence of Iron sulphate and hydrogen peroxide showed that orifice 3 had the best removal and was followed by orifice 2. Orange II concentration: 20 ppm, solution volume: 10 L, Iron sulphate: 100 mg, hydrogen peroxide: 10 mL, solution pH: 2, experiment time: 60 min. The sampling interval of 10 min, inlet pressure of 300 KPa, starting temperature 22°C.

The decolouration process in Figure 4.4 showed the effect of Fenton reagents (Iron and hydrogen peroxide) to the decolouration process in 4.1.1. The combined effect of the oxidising agent and the catalyst was predicted in theory to improve the decolouration process (Saharan et al., 2011). The outcome of this reaction showed otherwise, although the efficiency of removal kept a good trend. While the orifices OR2, OR3 and OR4 showed good decolouration, orifice OR6 was inefficient due to large orifice size. Based on the comparison between Figure 4.1 and Figure 4.4, it was recorded at 10 min that the orifices 2, 3, 4 and 6 mm that the percentage decolouration decreased respectively from 82 to 79%, 90 to 89%, 83 to 78% and 65 to 39%. This decrease can be attributed to an excessive amount of Fenton reagents causing a poor generation of hydroxyl radical, hence decreasing the percentage decolouration of orange II (Saharan et al., 2011). Slow decolouration can be assigned to the low generation rate of OH

radicals as a result of the slow reaction of complex iron which may be generated at pH > 4 in water or this can be due to the scavenging effect of hydrogen peroxide by excess protons (Badmus et al., 2018).

We have noted that most degradation were efficient below 10 min, therefore, the system should be optimised in that time frame for orifice alone since the throat of venturi produces almost no meaningful result.

4.1.2.4 Removal of Orange II using various orifices and venturi at 10 min

The decolouration of dye below 10 min using the same working conditions as in section 4.1.1 using various orifices (2, 3, 4, 5 and 6 mm). The same condition was maintained apart from the time which was shortened to 10 min with the sampling time which was shortened to 2 min apart.

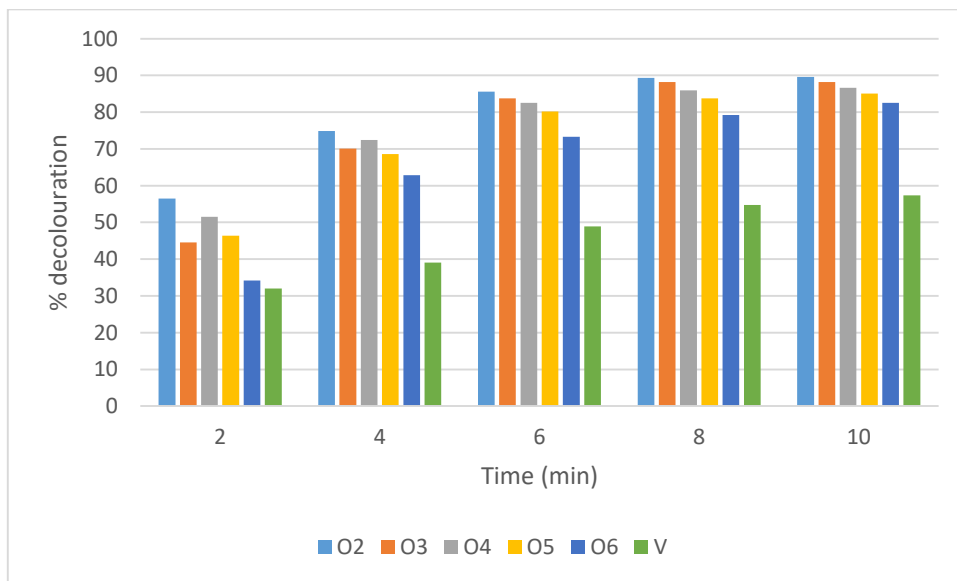


Figure 4.5 Impact of different cavitating devices (orifice and venturi) on dye decolouration in the HC pilot plant (Fixed parameters: Orange II concentration 20 ppm, solution volume 10 L, solution pH 2, experiment run for 10 min, sampling interval of 2 min, inlet pressure of 300 KPa, starting temperature 22°C

In Figure 4.5 above, the decolouration of dye at all the orifices size was achieved below 10 min. It had the highest percentage decolouration of orange II dye (90%) at 10 min for orifice 2 compare to orifice 3, 4, 5, 6 mm hole and the venturi which had respectively 88%, 87%, 85%, 83% and 57% decolouration rate. This can be attributed to the fact that small diameter single hole generates more cavitation intensity compare to large diameter single hole. As it was noticed in this study, as the diameter single hole increased from 2, 3, 4, 5 and 6 mm, the

percentage orange II dye decolouration decreased from 90%, 88%, 87%,85%, 83% respectively. However, the difference between these percentage decolouration is not significant. This could be due to the small difference in orifice single hole diameter size. The venturi decolouration rate below 10 min showed a positive decolouration. The venturi throat was 10 mm which makes the venturi perform poorly than then the 6 mm hole in decolouration.

4.1.2.5 Observed Hydrodynamic Cavitation under optimised conditions

The experiment below followed the same procedure as in section 4.1.2.4. The sampling also occurred at 2 min interval and below 10 min. the experiment was conducted for 2 mm orifice alone, for the venturi alone and the combination of orifice and the ventur to evaluate the three modes of dye decoloration.

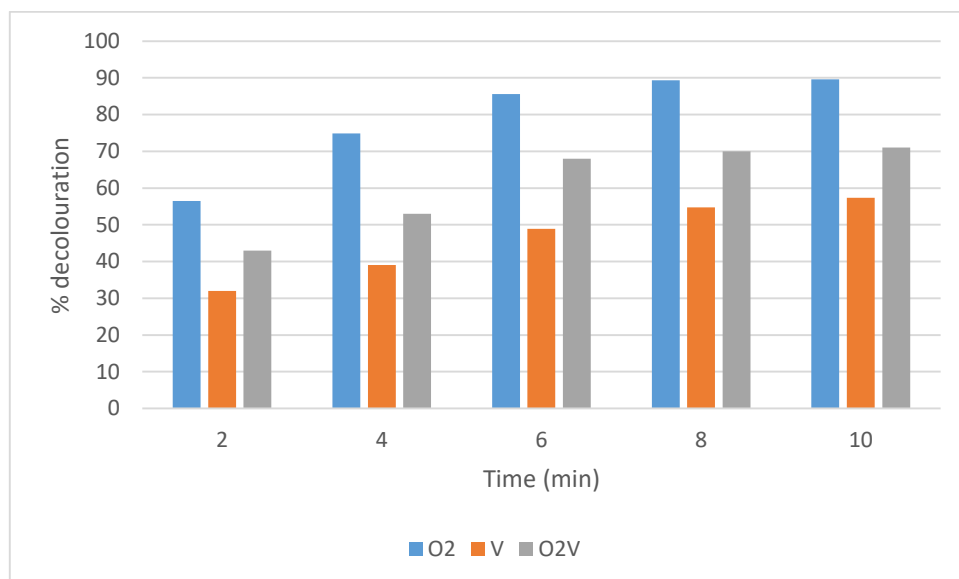


Figure 4.6 Effect of an orifice, a venturi and the combination of both cavitating devices on dye decolouration in the HC pilot plant (Fixed parameters: orifice 2 mm hole, Orange II concentration 20 ppm, solution volume 10 L, solution pH 2, experiment run for 10 min, sampling interval of 2 min, inlet pressure of 300 KPa, starting temperature 22°C)

The decolouration of orange II dye in Figure 4.6 was a comparative study of orifice, venturi and orifice and venturi. Orifice 2 mm proved to achieve the highest percentage decolouration on its own than in combination with the venturi. In a similar experiment, Gagol et al. (2018) found that the orifice with the smallest hole diameter provided a maximum rate of removal of triglycerides in a similar experience using Jet loop (Gagol et al., 2018). This can be assigned to many generated cavities. The cavitation event in this case limited the resistance of mass transfer while improving collapse (Lalwani et al., 2020). The venturi had a disadvantage of a

having a fixed throat size which was five times that of the selected orifice. It would thus not be expected to be better than the orifice decolouration. The combination of the two provided a trend that was reinforcing the observation that the combination of both techniques yielded a better result than the process with the venturi.

4.1.3 Removal of Perfluorooctanoic acid using optimum conditions

This experiment was conducted using the selected optimum conditions as outlined in section 4.1.2.4. The removal of PFOA occurred after completing the preparation in section 3.1.4. The selected experimental condition selected for dye under 10 min with a sampling time 2 min apart was selected. The orifice 2, 3, 4 and 6 mm size were used. The optimum condition obtained in the previous experiment were applied to the removal of Perfluorooctanoic acid namely 300 KPa pressure at the inlet, initial concentration of 20 ppm at pH 2 solution, initial temperature of 22°C and orifice 2 mm.

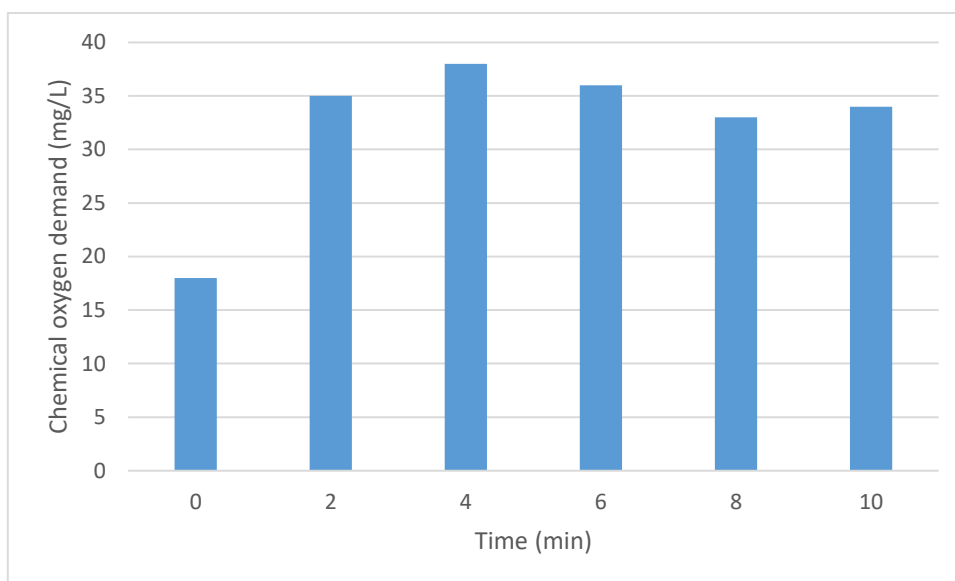


Figure 4.7 Chemical oxygen demand results for Perfluorooctanoic acid (Fixed parameters: orifice 2 mm hole, PFOA concentration 20 ppm, solution volume 10 L, solution pH 2, experiment run for 10 min, sampling interval of 2 min, inlet pressure of 300 KPa, starting temperature 22°C)

The result of monitoring the chemical oxygen demand (COD) demonstrated that the removal of PFOA was 18 mg/L. As time went on, the COD showed increased COD value while the successful removal would require that the COD value drops significantly. This resistance to removal is motivated by the structure of the PFOA. This was made up of fluorine ion which stabilised the compounds by inductive effects while the dye was compatible with the above

discussed methods of removal of dyes. For successful removal of COD, Vitez et al. (2012) provided 70 mg/L as a minimum efficiency value for removal of PFOA (Vitez et al., 2012). In this case, the removal of PFOA wasn't successful. Next to this reason, it can be highlighted that the limit of detection of an analytical instrument can affect its sensitivity as well as its accuracy. For instance, a sample having a concentration below the limit of detection of the instrument can induce a concern with the sensitivity of the analysis. When the sample is not properly diluted and the column blocked, this could cause irregularity in calibration and cause unreliable results (Foley & Dorsey, 1984).

4.2 Material Balance

4.2.1 Material balance calculations

Assumptions:

- The reaction occurred between Orange II and -OH free radicals but the -OH radicals produced were all consumed to form minerals (NaNO_3 , H_2SO_4 , Na_2CO_3) thus generation and consumption were cancelling each other, therefore were negligible.
- Steady state process, accumulation is 0 and what goes in comes out, thus there is conservation of mass.

The equation becomes:

$$d_m = m_{in} + G - m_{out} - G$$

$$0 = m_{in} - m_{out}$$

$$m_{in} = m_{out}$$

- The amount of orange II Sodium is negligible therefore the density of the mixture is equivalent to the density of the water.

Basis: Feed of 10 kg of the mixture fed to the system.

Overall material balance:

$$F = P$$

$$m_{WF} + m_{OR2F} = m_{WP} + m_{OR2P} = 10\text{kg}$$

$$X_{WF} + X_{OR2F} = X_{WP} + X_{OR2P} = 1$$

As the 20 ppm of orange II was prepared from 1000 ppm orange II, the volume of orange II in the feed was found from the equation: $C_1 V_1 = C_2 \cdot V_2$

with $C_1 = 1000\text{ppm}$, $C_2 = 20\text{ ppm}$, $V_2 = 10$ taken in the feed tank

$$V_{OR2F} = V_1 = \frac{20\text{ppm} \times 10\text{l}}{1000\text{ppm}} = 0.2\text{ l}$$

$$V_{WF} = 10\text{l} - 0.2\text{l} = 9.8\text{l}$$

$$m_{WF} = 9.8\text{l} \times 1000 \frac{\text{kg}}{\text{m}^3} \times \frac{1\text{m}^3}{1000\text{l}} = 9.8\text{ kg}$$

$$m_{OR2F} = 10\text{kg} - 9.8\text{kg} = 0.2\text{ kg}$$

$$X_{WF} = \frac{m_{WF}}{F} = \frac{9.8\text{kg}}{10\text{kg}} = 0.98$$

$$X_{OR2F} = \frac{m_{OR2F}}{F} = \frac{0.2\text{kg}}{10\text{kg}} = 0.02$$

Orange II was degraded from 20 ppm to 2.53 ppm at 10 min using orifice 2 mm diameter

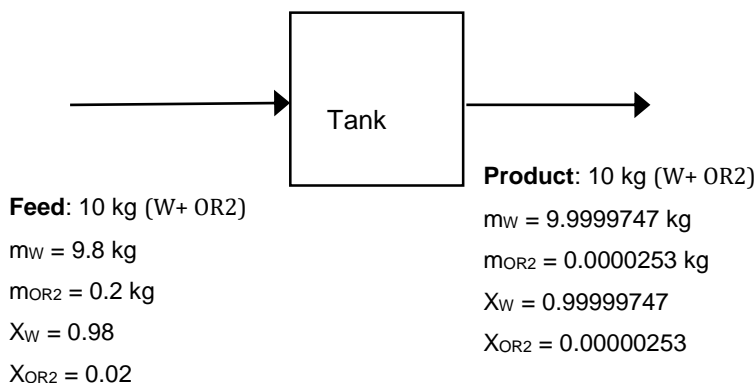
$$m_{OR2P} = C_{OR2P} \times V_P = 2.53 \frac{\text{g}}{\text{l}} \times 10\text{l} = 0.00253\text{g} \times \frac{1\text{kg}}{1000\text{g}} = 0.0000253\text{ kg}$$

$$m_{WP} = 10\text{ kg} - 0.0000253\text{kg} = 9.9999747\text{kg}$$

$$X_{WP} = \frac{m_{WP}}{P} = \frac{9.9999747\text{kg}}{10\text{kg}} = 0.99999747$$

$$X_{OR2P} = \frac{m_{OR2P}}{P} = \frac{0.0000253\text{kg}}{10\text{kg}} = 0.00000253$$

C, F, P, W, X represent concentration, feed, product, water and mass fraction respectively.



: **Table 4.1 Summary of the mole fraction of the component material balance around the tank**

Component	Input mole fraction	Output mole fraction
Water	0.98	0.99999747
Orange II Na salt	0.02	0.00000253
Total	1	1

Table 4.2 summary of component material balance around the tank

Component	Input	Output
Water	9.8 kg	9.9999747 kg
Orange II Na Salt	0.2 kg	0.0000253kg
Total	10 kg	10 kg

The mass entering and leaving the system were found through material balance and they were summarised in the table above. There was conservation of the total mass (10 kg) within the system. The material balance was evaluated using the following fixed parameters: orifice 2 mm hole, Orange II concentration 20 ppm, solution volume 10 L, solution pH 2, experiment run for 10 min, sampling interval of 2 min, inlet pressure of 300 KPa, starting temperature 22°C

4.3 Chemical kinetics

The determination of the order of reaction for the degradation of orange II dye solution is important. In this study, 20 ppm orange II dye solution was represented by reactant A. The order of reaction was found using an integration method based on the optimum conditions results which were obtained using orifice 2 mm (O2), the venturi (V) and the combination of orifice 2 mm and the venturi (O2V).

The figures below represent the plot of the zero, first and second order reaction at the optimum conditions.

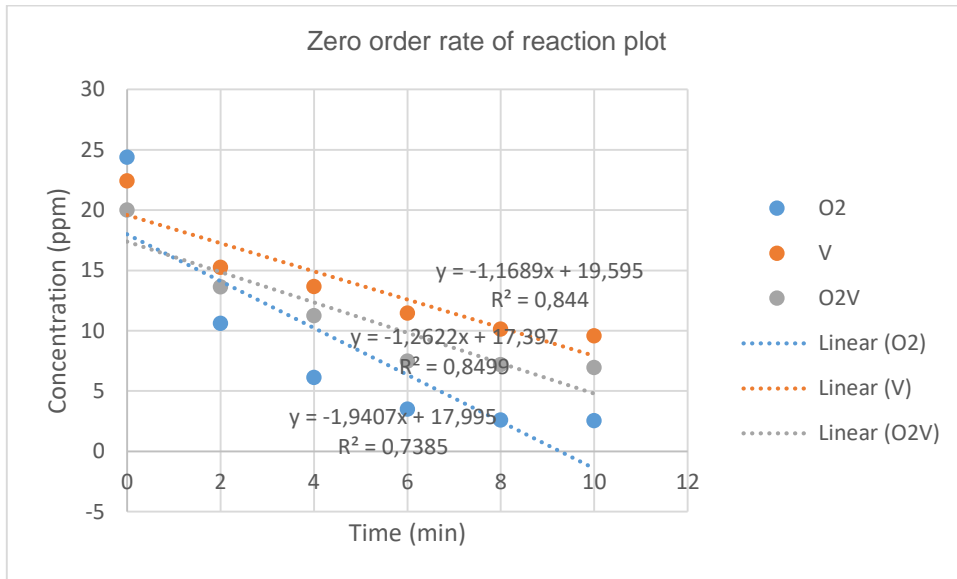


Figure 4.8 Zero-order rate of reaction for removal of orange II using optimised conditions (Fixed parameters: orifice 2 mm, Orange II concentration 20 ppm, solution volume 10 L, solution pH 2, experiment run for 10 min, sampling interval of 2 min, inlet pressure of 300 KPa, starting temperature 22°C)

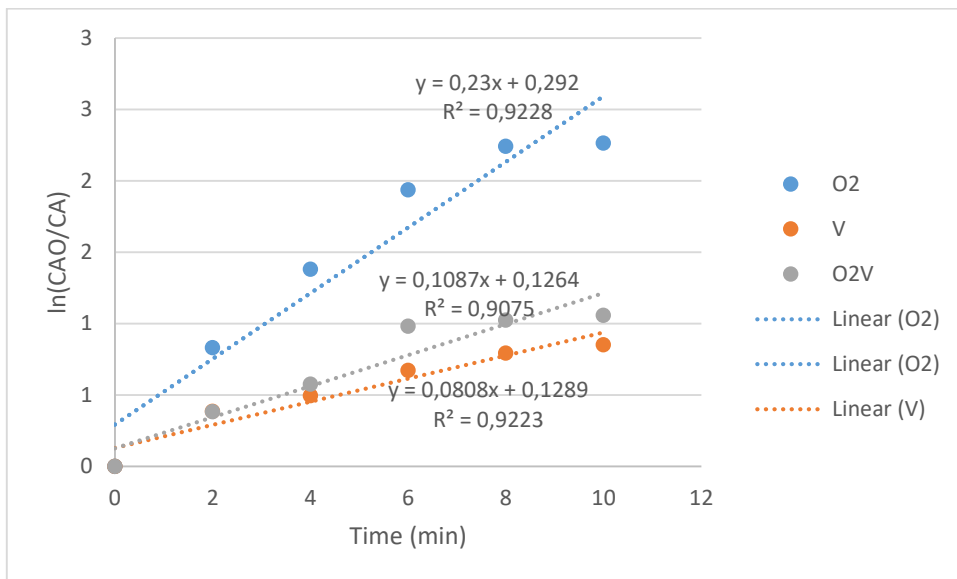


Figure 4.9 First order rate reaction plot for removal of orange II using optimised conditions (Fixed parameters: orifice 2 mm, Orange II concentration 20 ppm, solution volume 10 L, solution pH 2, experiment run for 10 min, sampling interval of 2 min, inlet pressure of 300 KPa, starting temperature 22°C)

With CAO being the initial concentration of orange II and CA concentration at a given time t.

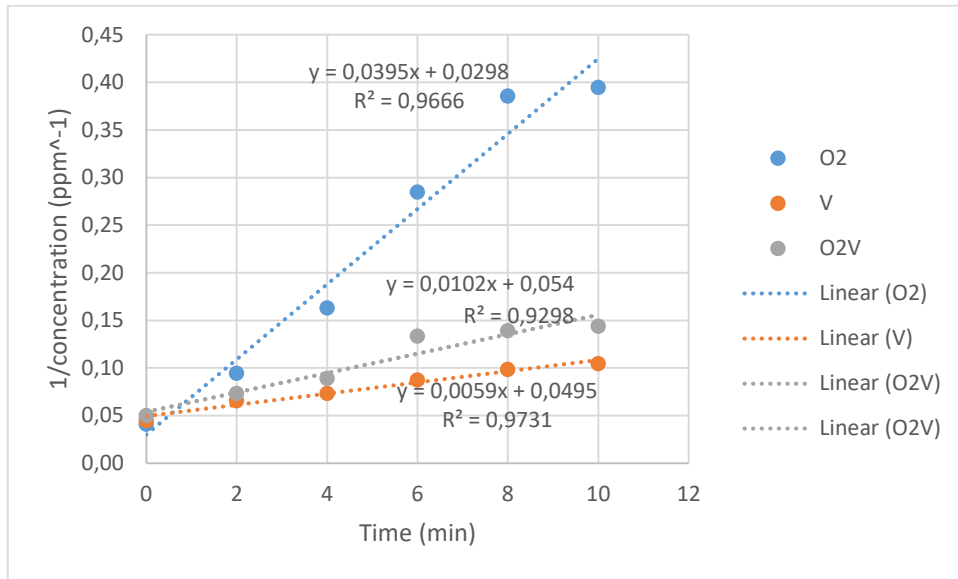


Figure 4.10 Second order rate of reaction plot for removal of orange II using optimised conditions (Fixed parameters: orifice 2 mm, Orange II concentration 20 ppm, solution volume 10 L, solution pH 2, experiment run for 10 min, sampling interval of 2 min, inlet pressure of 300 KPa, starting temperature 22°C)

The plots of orifice 2 mm (O2), venturi (V) as well as combination of orifice 2 mm and venturi (O2V) showed respectively that the reaction is second order with the highest regression coefficient R^2 and the slope equal to 0.966 and 0.0395 L/ mg min respectively (orifice 2 mm diameter); 0.9266 and 0.0102 L/mg min (venturi) and 0.9731 and 0.0059 L/ mg min (orifice 2 mm diameter and the venturi). However, due to no change in the concentration in water, the reaction has a tendency to respond like a first order with regression coefficient R^2 and the slope respectively equal to 0.9228 and 0.23 min^{-1} using orifice 2 mm diameter; 0.9075 and 0.1087 min^{-1} using venturi and 0.9223 and 0.0808 min^{-1} using the combination of both orifice 2 mm diameter and the venturi. Therefore, the reaction is pseudo first-order, the rate of decolourisation of orange II of 0.23 min^{-1} is directly proportional to the concentration of orange II according to first order kinetics and it is given by $-r = k[C_{OR2}] = 0.23 \text{ min}^{-1}[C_{OR2}]$ (using orifice 2 mm). C stands for the concentration of dye in mole/l, k represents the rate constant (min^{-1}) and t is the time in minutes.

Badmus (2019) and Wang et al. (2009) confirmed in their work that dye decolourisation with HC pilot plant followed a pseudo first-order law. Badmus's experimental run employed two orifices in an hour-long experiment on the HC pilot plant. Both the two orifices and venturi had a 4 mm diameter and were aligned parallel to each other. Wang et al (2019) made use of a jet

loop cavitation device for 1.5 h to reach the same conclusion as Badmus (2009) (Badmus, 2019), and Wang et al. (2009) (Wang et al., 2009).

4.4 Energy balance around HC pilot plant

Energy balance calculations

Figure 4.11 below represents the system on which the energy balance was performed.

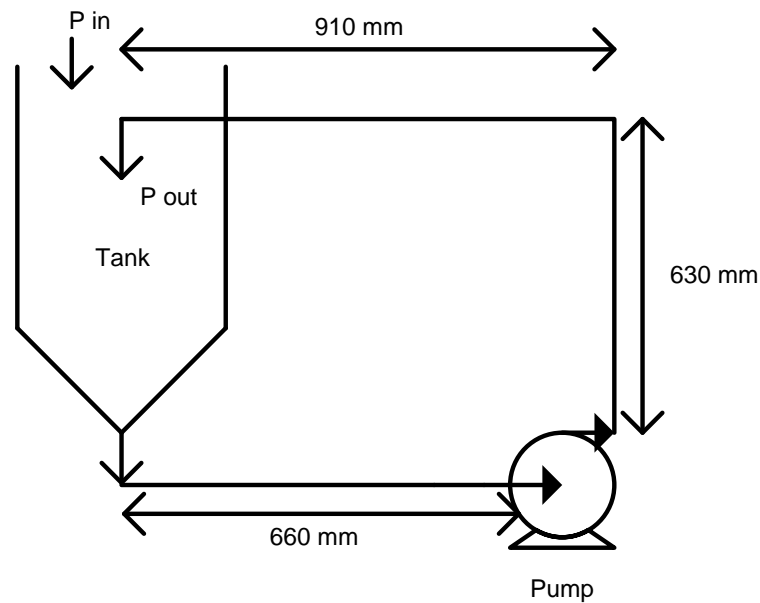


Figure 4.11 Process flow diagram of HC reactor

Assumptions

- Steady state, so that the rate of energy accumulation $\frac{dE_k}{dt} + \frac{dE_P}{dt} + \frac{dU}{dt} = 0$; the inlet mass flowrate \dot{m}_{in} is equal to the outlet mass flowrate \dot{m}_{out} ; the inlet specific heat capacity $C_{P_{in}}$ is equal to the outlet specific heat capacity $C_{P_{out}}$
- The system has only a single inlet and a single outlet. Thus equation (5) becomes:

$$0 = \dot{m} \left(C_P (T_{in} - T_{ref}) + \frac{v_{in}^2}{2} + gz_{in} - C_P (T_{out} - T_{ref}) - \frac{v_{out}^2}{2} - gz_{out} \right) + \dot{Q} - \dot{W}_s \quad (6)$$

$$\dot{m} \left(C_P (T_{out} - T_{in}) + \frac{v_{out}^2 - v_{in}^2}{2} + g(z_{out} - z_{in}) \right) - \dot{Q} = -\dot{W}_s \quad (7)$$

$$\dot{m} \left(C_P (T_{out} - T_{in}) + \frac{v_{out}^2 - v_{in}^2}{2} + g(z_{out} - z_{in}) - Q \right) = -\dot{W}_s \quad (8)$$

- No phase change

- No other sources of large amounts of heat transfer
- The heat generated ($-Q$) was due to friction in the pipes and fittings. It is called friction loss and can be represented by F , thus equation (8) can be written as:

$$\dot{m} \left(C_p(T_{out} - T_{in}) + \frac{v_{out}^2 - v_{in}^2}{2} + g(z_{out} - z_{in}) + F \right) = -\dot{W}_s \quad (9)$$

- The inlet velocity v_{in} is negligible thus $v_{in} = 0$
- $z_{in} = 0$ as it is taken as the reference for elevation
- The density, the specific heat capacity, and the viscosity of solution were equal to the density, the specific heat capacity, and the viscosity of water since the solution is made of a large amount of water and the amount of orange II dye was negligible to affect the specific heat capacity, the density and the viscosity of solution.
- The flow is incompressible, so the density of the solution is constant thus the specific inlet volume is equal to the specific outlet volume given by $\dot{V}_{in} = \dot{V}_{out} = \frac{1}{\rho}$

Table 4.3 : Energy balance calculation constants

Mass (m)	10 kg	
Experimental running time (t)	10 min	
Gravitational acceleration (g)	9.8 m/s ²	
Outlet elevation (z _{out})	630 mm	
Diameter (d)	25 mm	
Length (L)	2200 mm	
Specific heat capacity of water (C _p)	4184 J/kg °C	
Density of water (ρ)	1000 kg/m ³	
Viscosity of water (μ)	0.001 Pa.s	
Electric power of the pump	2.2 kW	
Fitting or valve type	Quantity	Velocity head constant (k)
Pipe entry	1	1
One 90°elbow	2	0.75
Ball valve	2	70
Pipe exit	1	0.5

The mass flowrate, the temperature rise, the outlet velocity and the friction loss were calculated in order to determine the shaft work performed by the pump.

The mass flow rate is given by $\dot{m} = \frac{m}{t} = \frac{10 \text{ kg}}{10 \text{ min}} \times \frac{1 \text{ min}}{60 \text{ s}} = 0,0167 \text{ kg/s}$

The increase in temperature of a specified fluid quantity of 10 L was monitored at the pressure inlet of 300 KPa every 2 min and the obtained data were plotted depicted in Figure 4.12

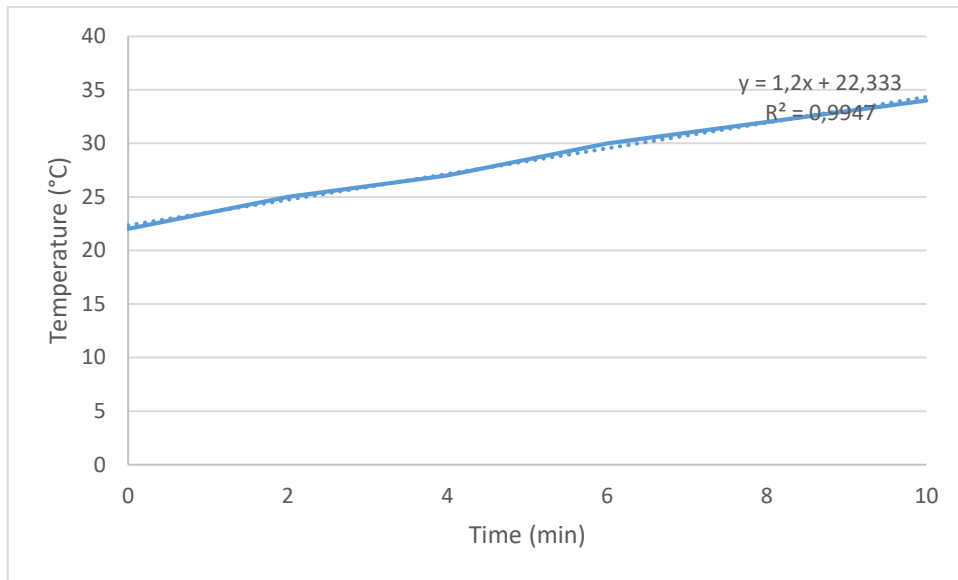


Figure 4.12 Temperature rise profile (Fixed parameters: orifice 2 mm hole, Orange II concentration 20 ppm, solution volume 10 L, solution pH 2, experiment run for 10 min, sampling interval of 2 min, inlet pressure of 300 KPa, starting temperature 22°C)

The observed $\frac{dT}{dt} = \frac{1,2^\circ\text{C}}{\text{min}}$

$$T_{out} - T_{in} = dT = \frac{1,2^\circ\text{C}}{\text{min}} \times 10 \text{ min} = 12^\circ\text{C}$$

The outlet velocity is given by $v = \frac{\dot{V}}{A}$

The volumetric flowrate is given by $\dot{V} = \frac{\dot{m}}{\rho} = \frac{0,0167 \text{ kg/s}}{1000 \text{ kg/m}^3} = 0,0000167 \text{ m}^3/\text{s}$

The outlet area is given by $A = \pi \frac{d^2}{4} = \pi \frac{(0,025 \text{ m})^2}{4} = 0,000491 \text{ m}^2$

$$\text{Thus } v = \frac{0,0000167 \text{ m}^3/\text{s}}{0,000491 \text{ m}^2} = 0,0340 \text{ m/s}$$

The friction loss \dot{F} is given by $\dot{F} = f \frac{L}{d} \frac{v^2}{2} + \sum k \frac{v^2}{2}$ with $f, L, v, d, \sum k$ and \dot{m} representing respectively the friction factor, the length, the velocity, the diameter and the sum of friction factor

The friction factor (f) is given by $f = \frac{64}{Re}$ for laminar flow when the Reynold (Re) number is less than 4100, for turbulent flow with Reynold number greater than 4100, the friction factor is found from the intercept between the Re and the relative roughness (ϵ) in the moody chart.

The relative roughness is given by $\epsilon = \frac{\epsilon}{d}$ with ϵ and d representing the absolute roughness of the material and the diameter of the pipe respectively.

Reynold number is given by $Re = \frac{\rho v d}{\mu}$ with ρ, v, d and μ representing the density, the velocity, the diameter and the viscosity of the fluid respectively.

$Re = \frac{1000 \text{ kg/m}^3 \times 0.0340 \text{ m/s} \times 0.025 \text{ m}}{0.001 \text{ Pa s}} = 850$ which is smaller than 4100, therefore the flow is laminar (Geankoplis, 1993).

Thus, $f = \frac{64}{850} = 0.0753$ (Appendix B)

The sum of velocity head is given by $\sum k = \sum N_f \times k_f$ with N_f and k_f representing the quantity and the velocity head of fittings respectively.

$$\sum k = 1 \times 1 + 2 \times 1.5 + 2 \times 70 + 1 \times 0.5 = 143$$

$$\text{Thus, } F = 0.0753 \times \frac{2.2 \text{ m}}{0.025 \text{ m}} \times \frac{(0.0340 \text{ m/s})^2}{2} + 143 \times \frac{(0.0340 \text{ m/s})^2}{2} = 0.0865 \frac{\text{m}^2}{\text{s}^2} = 0.0865 \text{ J/kg}$$

The shaft work exerted by the pump is given by

$$-\dot{W}_s = \dot{m} \left(C_p (T_{out} - T_{in}) + \frac{v_{out}^2 - v_{in}^2}{2} + g(z_{out} - z_{in}) + F \right)$$

$$\text{Thus, } -\dot{W}_s = 0.0167 \text{ kg/s} \times \left(4184 \frac{\text{J}}{\text{kg}^\circ\text{C}} \times 12^\circ\text{C} + \frac{\left(\frac{0.034 \text{ m}}{\text{s}}\right)^2 - 0^2}{2} + 9.8 \text{ m/s}^2 (0.63 \text{ m} - 0) + 0.0865 \text{ J/kg} \right)$$

$$-\dot{W}_s = 0.0167 \text{ kg/s} \times \left(50208 \frac{\text{J}}{\text{kg}} + 0.00116 \frac{\text{J}}{\text{kg}} + 6.174 \frac{\text{J}}{\text{kg}} + 0.0865 \frac{\text{J}}{\text{kg}} \right)$$

$$-\dot{W}_s = 838.4736 \text{ W} + 0.0000194 \text{ W} + 0.1031058 \text{ W} + 0.0014446 \text{ W}$$

$$-\dot{W}_s = 839 \text{ W} = 0.839 \text{ KW}$$

The energy required in the pump for the production of cavities which collapse and produce OH free radicals for removal of 20 ppm orange II in 10 L solution volume resulting in 90 % decolourisation of orange II dye was 0.839 KW.

The results of the energy balance calculation showed that in HC the change in kinetic energy, potential energy and the friction losses are negligible. The increase in temperature per unit time due to friction and pressure pulses due to cavities collapse were the most predominant form of energy as the chemical and physical effects of cavitation were monitored (Shah et al., 1999).

This confirms what Gogate, 2001 and Thanekar et al., 2021 said about the calculation of energy efficiency in the HC reactor which is found using a calorimetry study with the actual power dissipated in the system given by $P \text{ (Watt)} = mC_p \frac{dT}{dt}$ over the supplied electrical power, where, m represents the mass of fluid circulating in the system (kg), C_p represents the heat capacity, J/Kg °C; dT/dt represents the rate at which temperature changes with respect to time.

Shah et al. (1999) also stated that the cavitation power entering the reactor is not always the same as electrical power consumed. Cavitation power is monitored using a calorimeter with the measurement of the initial temperature change at the beginning of the process.

$$\text{Energy efficiency (\%)} = \frac{0.839 \text{ KW}}{2.2 \text{ KW}} \times 100 = 38 \%$$

The efficiency of hydrodynamic cavitation with displacement pump (high pressure) equipment falls between 20 and 40% with flow range smaller than 10 m³/h (Shah et al., 1999). In this study, the efficiency found was between 20 and 40% and the flow rate ($0.0000167 \frac{\text{m}^3}{\text{s}} \times \frac{3600 \text{ s}}{1 \text{ h}} = 0.0601 \text{ m}^3/\text{h}$) was smaller than 10 m³/h.

Energy efficiency based on cavitation yield was given by:

$$\text{Cavitation yield} \left(\frac{\text{mg}}{\text{L}} \right) = \frac{\left(\frac{90}{100} \right) \times 20 \text{ mg/L}}{\left(2200 \text{ W} \times 10 \text{ min} \times \frac{60 \text{ s}}{1 \text{ min}} \right) \times 10 \text{ L}} = 1.36 \times 10^{-4} \text{ mg/J}$$

4.5 Cost

4.5.1 Cost estimation calculations

In this study, capital cost investment was estimated using a detailed factorial estimate.

The Assumptions were:

- The major equipment used in the HC pilot plant are a tank and a pump.
- Cost for building process, utilities services (provision on plant in firefighting equipment, air, steam and water services), storage (for both raw materials and finished product), site development, ancillary building (offices, laboratory buildings, workshops), contingency are not included in the total cost of HC pilot plant.
- The working capital cost represent 15% of the fixed capital cost.

Equipment	Capacity	Price	Reference
Tank	200 L	R 2131.008	Alibaba, 2021
Centrifugal Pump	2.2 KW, 400 V	R 6 098.45	Agrico, 2021

The price of a 80 L tank is given by: $C_{T80} = R\ 2\ 131.008 \times \left(\frac{80\ L}{200\ L}\right)^{0.6} = R\ 1\ 229.8$

$$PCE = R\ 1\ 229.8 + R\ 6\ 098.45 = R\ 7\ 328.25$$

The direct cost items included in the total cost of the HC pilot plant are equipment erection f_1 , piping f_2 , instrumentation f_3 and electrical f_4 .

$$PPC = PCE(1 + f_1 + f_2 + f_3 + f_4)$$

$$PPC = R\ 7\ 328.25 (1 + 0.40 + 0.70 + 0.20 + 0.10) = R\ 17\ 587.8$$

The indirect cost added to the direct cost are design and engineering f_{10} and contractor's fees f_{11} . Thus, fixed capital = $PPC(1 + f_{10} + f_{11})$

$$\text{Fixed capital} = R\ 17\ 587.8 (1 + 0.30 + 0.05) = R\ 23\ 743.53$$

$$\text{Working capital cost} = 0.15(R\ 23\ 743.53) = R\ 3\ 561.5$$

$$\text{Total capital investment needed} = R\ 23\ 743.53 + R\ 3\ 561.5 = R\ 27\ 305$$

4.3.4.2. Operating cost

The operating cost considered in this study involved the cost of raw materials and utilities. The raw material consisted of the simulated wastewater and the sulphuric acid used to adjust the pH of wastewater. The utilities consisted of tap water and electricity. Tap water was used to rinse HC pilot plant before running the experiment and electricity was used to operate HC pilot plant.

- Cost of raw materials

Table 4.4 Raw materials prices

Raw materials	Price	Reference
Wastewater	Free	N/A
Sulphuric acid	R 401/500mL	Sigma-Aldrich, 2021

The cost of sulphuric acid (H_2SO_4) is given by the amount of sulphuric acid (10 mL) used multiplied by the price of sulphuric acid = $10 \text{ mL} \times \frac{R 401}{500 \text{ mL}} = R 8.02$

- Cost of utilities

Table 4.5 Utilities prices

Utilities	Price	Reference
Tap Water	R 32.65/1000L	(Department, 2017)
Electricity	R 1.0384/KWh	(Jurgilewicz & Poplavska, 2019)

The operation cost of HC pilot plant (C) is given by $C = EP^*$ with E representing energy used by HC pilot plant in kWh/m^3 and P^* the price of electricity in $R \text{ kWh}^{-1}$

$$E = 839 \text{ W} \times \frac{1 \text{ kW}}{1000 \text{ W}} \times 10 \text{ min} \times \frac{1 \text{ h}}{60 \text{ min}} \times \frac{1}{10 \text{ L}} \times \frac{1000 \text{ L}}{\text{m}^3} = 14 \text{ kWh}/\text{m}^3$$

$$E = 839 \text{ W} \times \frac{1 \text{ kW}}{1000 \text{ W}} \times \frac{1 \text{ h}}{60 \text{ min}} \times 10 \text{ min} = 0.14 \text{ kWh}$$

$$C_E = \frac{14 \text{ kWh}}{\text{m}^3} \times \frac{R 1.0384}{\text{kWh}} = R 14.5376/\text{m}^3$$

$$\text{The cost of treatment of } 10 \text{ L} = \frac{R 14.5376}{\text{m}^3} \times 10 \text{ L} \times \frac{1 \text{ dm}^3}{1 \text{ L}} \times \frac{1 \text{ m}^3}{1000 \text{ dm}^3} = 0.145 \text{ R}$$

$$\text{Assuming the amount of water used was } 20 \text{ L, the cost of water is given by: } C_W = 20 \text{ L} \times \frac{R 32.65}{1000 \text{ L}} = R 0.653$$

Cost of water used is given by the amount of water used (20 L) multiplied by the price of water

$$\text{The total operating cost of HC process over a period of } 10 \text{ min} = R 8.02 + R 0.653 + R 0.145 = R 8.82$$

5. CHAPTER 5. GENERAL CONCLUSIONS AND RECOMMENDATIONS

In this study, the efficiency of orifice single hole of various diameters was successfully investigated on the removal of the selected persistent contaminant (dyes). The efficiency of orifice 2 mm hole diameter was found to be ideal at 90 % decolouration of orange II dye compare to efficiency of orifice 3, 4, 5 and 6 mm which yielded 88 %, 87 %, 85 % and 83 % respectively between 0 and 10 min. This can be due to the fact that small orifice diameter generates high cavitation intensity because of high pressure recovery. The efficiency of the venturi on the removal of orange II dye was evaluated and yielded at 10 min 57 % decolouration of orange II which was lower compare to the percentage decolouration yielded by different orifice diameter hole. This can be attributed to the fact that the 10 mm venturi diameter throat is big compare to 2, 3, 4, 5 and 6 mm orifice diameter hole, hence venturi generates low cavitation intensity due to low pressure recovery and low flow rate at the 10 mm constriction.

The efficiency of combined orifice hole and the venturi was assessed using orifice 2 mm hole which yielded a high percentage decolouration of orange II. The combination of orifice 2 mm hole and the venturi yielded 71 % degradation of orange II which is higher compared to the percentage decolouration of orange II obtained when using the venturi. However, the efficiency of combined orifice 2 mm and the venturi is lower compared to when using orifice 2 mm alone. This can be due to the fact of low cavitation intensity in the combined orifice and venturi resulting in low pressure recovery.

The impact of various operating parameters such as contact time, catalyst, oxidizing agent and Fenton reagents was investigated. Orange II was first run alone, then with iron, with hydrogen peroxide and with both Fenton and hydrogen peroxide for 60 min using 10 min interval time for sampling. It was found that there was a high decolouration of orange II between 0 and 10 min for all experiments. After 10 min, the percentage decolouration was changing with a small gradient so that the run using Fenton reagent had the larger gradient compared to the experiment with none of the elements. This is assigned to the fact that the effect of iron, hydrogen peroxide, Fenton reagents slightly increase the percentage decolouration. The catalyst wasn't very efficient at decolouration because it wasn't optimised. In fact, the amount of iron II involved was excessive causing poor decolouration and drop in the potential of hydroxyl radicals resulting in low decolouration.

The material and energy balances were performed on the HC pilot plant. The masses entering and leaving the system were determined. There was no creation nor loss of mass, the total mass was conserved. The energy consumption of the HC pilot plant was found to be 839 W and the energy efficiency was found to be 38 % or $1.36 \times 10^{-4} \text{mg/J}$. This can be attributed to the change in temperature from 22°C to 34°C which induced cavitation, the high pressure and the low flow rate of the sample. The cost estimation of capital investment, the operating cost as well as the cost of operating the plant for the decolouration of orange II was calculated to determine the required amount of money to set up the plant. Chemical kinetics were evaluated and the rate flow was 0.23 min^{-1} . The order of the reaction was pseudo first order, it was found that the HC system using orifice 2 mm hole took 10 min time to achieve 90% decolouration of orange II and the reaction was first order, which meant the concentration of orange II increases by a factor of 2 as the rate would increase by the same factor. The cost estimation of capital investment and operating cost was done to determine the cost to set up the plant and the cost of operating the plant for the decolouration of orange II. The capital investment and operating cost were found to be R 27 305 and R 8.82 for 10L of per sample respectively. The removal of perfluorooctanoic acid was ineffective using hydrodynamic cavitation, in the operation time this could be due to the PFOA chemical structure which did not allow it to follow Beer Lambert law as a result of excessive electron withdrawing group which the PFOA turn easily into its conjugate base.

REFERENCE

- Abdel-Raouf, M.E., Maysour, N., Farag, R.K. & Abdul-Raheim, M. 2019. Wastewater treatment methodologies. review article international. *Journal of Environment & Agricultural Science Wastewater Treatment Methodologies, Review Article. International Journal of Environment & Agricultural Science*, 3(1): 1–25.
- Akhtar, M.F., Ashraf, M., Javeed, A., Anjum, A.A., Sharif, A., Saleem, A., Akhtar, B., Khan, A.M. & Altaf, I. 2016. Toxicity Appraisal of Untreated Dyeing Industry Wastewater Based on Chemical Characterization and Short Term Bioassays. *Bulletin of Environmental Contamination and Toxicology*, 96(4): 502–507.
- Akpor, O. & Muchie, M. 2015. Environmental and public health implications of wastewater quality. , (June).
- Badmus, K.O. 2019. *Treatment of persistent organic pollutants in wastewater with combined advanced oxidation*. University of the Western Cape.
- Badmus, K.O., Irakoze, N., Adeniyi, O.R. & Petrik, L. 2020. Synergistic advance Fenton oxidation and hydrodynamic cavitation treatment of persistent organic dyes in textile wastewater. *Journal of Environmental Chemical Engineering*, 8(2): 103521.
- Badmus, K.O., Tijani, J.O., Eze, C.P., Fatoba, O.O. & Petrik, L.F. 2016. Quantification of Radicals Generated in a Sonicator. *Analytical and Bioanalytical Chemistry Research*, 3(1): 139–147.
- Badmus, K.O., Tijani, J.O., Massima, E. & Petrik, L. 2018. Treatment of persistent organic pollutants in wastewater using hydrodynamic cavitation in synergy with advanced oxidation process. *Environmental Science and Pollution Research*, 25(8): 7299–7314.
- Bagal, M. V. & Gogate, P.R. 2014. Degradation of diclofenac sodium using combined processes based on hydrodynamic cavitation and heterogeneous photocatalysis. *Ultrasonics Sonochemistry*, 21(3): 1035–1043.
- Bagal, M. V & Gogate, P.R. 2013. Ultrasonics Sonochemistry Degradation of diclofenac sodium using combined processes based on hydrodynamic cavitation and heterogeneous photocatalysis. *ULTRASONICS SONOCHEMISTRY*.
- Behera, S., Ghanty, S., Ahmad, F., Santra, S. & Banerjee, S. 2012. UV-Visible Spectrophotometric Method Development and Validation of Assay of Paracetamol Tablet Formulation. *Journal of Analytical & Bioanalytical Techniques*, 3(6): 151–156.
- Benkhaya, S., Souad, M. & Harfi, A. El. 2020. A review on classifications, recent synthesis and applications of textile dyes. *elsevier*.
- Berradi, M., Hsissou, R., Khudhair, M., Assouag, M., Cherkaoui, O., El Bachiri, A. & El Harfi, A. 2019. Textile finishing dyes and their impact on aquatic environs. *Heliyon*, 5(11): 785–793.
- Braeutigam, P., Franke, M., Wu, Z.L. & Ondruschka, B. 2010. Role of different parameters in the optimization of hydrodynamic cavitation. *Chemical Engineering and Technology*, 33(6): 932–940.
- Chakinala, A.G., Gogate, P.R., Burgess, A.E. & Bremner, D.H. 2009. Industrial wastewater treatment using hydrodynamic cavitation and heterogeneous advanced Fenton processing. *Chemical Engineering Journal*, 152(2–3): 498–502.
- Chakinala, A.G., Gogate, P.R., Burgess, A.E. & Bremner, D.H. 2008. Treatment of industrial wastewater effluents using hydrodynamic cavitation and the advanced Fenton process. *Ultrasonics Sonochemistry*, 15(1): 49–54.
- Chiong, T., Lau, S.Y., Lek, Z.H., Koh, B.Y. & Danquah, M.K. 2016. Enzymatic treatment of methyl orange dye in synthetic wastewater by plant-based peroxidase enzymes. *Journal of Environmental Chemical Engineering*, 4(2): 2500–2509. <http://dx.doi.org/10.1016/j.jece.2016.04.030>.
- Concerns, E. 2013. *The Environmental, Health and Economic Impacts of Textile Azo Dyes*. Department, W. and S. 2017. Water and sanitation department. , 17(Annexure 6): 2.

- <http://www.capetown.gov.za/Departments/Water and Sanitation Department>.
- Dular, M., Griessler-Bulc, T., Gutierrez-Aguirre, I., Heath, E., Kosjek, T., Krivograd Klemenčič, A., Oder, M., Petkovšek, M., Rački, N., Ravnikar, M., Šarc, A., Širok, B., Zupanc, M., Žitnik, M. & Kompare, B. 2016. Use of hydrodynamic cavitation in (waste)water treatment. *Ultrasonics Sonochemistry*, 29(Volume): 577–588.
- European Union Policy, E. 2017. *Science for Environment Policy Future Brief: Persistent organic pollutants: towards a POPs-free future*.
- Foley, J.P. & Dorsey, J.G. 1984. Clarification of the limit of detection in chromatography. *Chromatographia*, 18(9): 503–511.
- Gadipelly, C., Pérez-González, A., Yadav, G.D., Ortiz, I., Ibáñez, R., Rathod, V.K. & Marathe, K. V. 2014. Pharmaceutical industry wastewater: Review of the technologies for water treatment and reuse. *Industrial and Engineering Chemistry Research*, 53(29): 11571–11592.
- Gągol, M., Przyjazny, A. & Boczkaj, G. 2018. Wastewater treatment by means of advanced oxidation processes based on cavitation – A review. *Chemical Engineering Journal*, 338(November 2017): 599–627.
- Geankoplis, C.J. 1993. *Transport Processes and Unit Operations*. 3rd Editio. New Jersey: Prentice Hall International.
- Gogate, P.R. 2007. Application of cavitation reactors for water disinfection: Current status and path forward. *Journal of Environmental Management*, 85(4): 801–815.
- Gogate, P.R. & Bhosale, G.S. 2013. Comparison of effectiveness of acoustic and hydrodynamic cavitation in combined treatment schemes for degradation of dye wastewaters. *Chemical Engineering and Processing: Process Intensification*, 71: 59–69. <http://dx.doi.org/10.1016/j.cep.2013.03.001>.
- Gogate, P.R., Shirgaonkar, I.Z., Sivakumar, M., Senthilkumar, P., Vichare, N.P. & Pandit, A.B. 2001. Cavitation reactors: Efficiency assessment using a model reaction. *AIChE Journal*, 47(11): 2526–2538.
- Gogate, P.R., Tayal, R.K. & Pandit, A.B. 2006. Cavitation: A technology on the horizon. *Current Science*, 91(1): 35–46.
- Gore, M.M., Saharan, V.K., Pinjari, D. V., Chavan, P. V. & Pandit, A.B. 2014. Degradation of reactive orange 4 dye using hydrodynamic cavitation based hybrid techniques. *Ultrasonics Sonochemistry*, 21(3): 1075–1082. <http://dx.doi.org/10.1016/j.ultsonch.2013.11.015>.
- HACH. 2010. Dr/2010 spectrophotometer. *Test*.
- Innocenzi, V., Prisciandaro, M., Tortora, F. & Vegliò, F. 2018. Optimization of hydrodynamic cavitation process of azo dye reduction in the presence of metal ions. *Journal of Environmental Chemical Engineering*, 6(6): 6787–6796. <https://doi.org/10.1016/j.jece.2018.10.046>.
- ITRC. 2018. Naming Conventions and Physical and Chemical Properties of Per- and Polyfluoroalkyl Substances. *Interstate technology regulatory council*: 1–15.
- Jain, T., Carpenter, J. & Saharan, V.K. 2014. CFD Analysis and Optimization of Circular and Slit Venturi for Cavitation Activity. *Journal of Material Science and Mechanical Engineering (JMSME)*, 1(1): 28–33. <http://www.krishisanskriti.org/jmsme.html>.
- Jurgilewicz, O. & Poplavska, Z. 2019. JOURNAL OF SECURITY AND SUSTAINABILITY ISSUES. , 9(2): 199–212.
- Kant, R. 2012. Textile dyeing industry an environmental hazard. *Natural Science*, 04(01): 22–26.
- Karl Kolmetz. 2014. Kolmetz Handbook of Process Equipment Design SAFETY IN PROCESS EQUIPMENT DESIGN (ENGINEERING DESIGN GUIDELINE). , (June 2014): 1–22.
- Katheresan, V., Kansedo, J. & Lau, S.Y. 2018. Efficiency of various recent wastewater dye removal methods: A review. *Journal of Environmental Chemical Engineering*, 6(4): 4676–4697.
- Kumar, M.S., Sonawane, S.H., Bhanvase, B.A. & Bethi, B. 2018. Treatment of ternary dye

- wastewater by hydrodynamic cavitation combined with other advanced oxidation processes (AOP's). *Journal of Water Process Engineering*, 23(March): 250–256. <https://doi.org/10.1016/j.jwpe.2018.04.004>.
- Kunacheva, C., Senevirathna, S.T.M.L.D., Tanaka, S., Fujii, S., Lien, N.P.H., Nozoe, M. & Shivakoti, B.R. 2011. The emergence of persistent organic pollutants in the environment : the occurrence and treatment of perfluorinated compounds. *SANSAI : An Environmental Journal for the Global Community*, 5(September 2015): 37–50.
- Lalwani, J., Gupta, A., Thatikonda, S. & Subrahmanyam, C. 2020. Oxidative treatment of crude pharmaceutical industry effluent by hydrodynamic cavitation. *Journal of Environmental Chemical Engineering*, 8(5).
- Li, J., Luo, G., He, L.J., Xu, J. & Lyu, J. 2018. Analytical Approaches for Determining Chemical Oxygen Demand in Water Bodies: A Review. *Critical Reviews in Analytical Chemistry*, 48(1): 47–65.
- Malato, S. 2008. Removal of emerging contaminants in waste-water treatment: Removal by photo-catalytic processes. *Handbook of Environmental Chemistry, Volume 5: Water Pollution*, 5 S2(November 2007): 177–197.
- Material, S. 1899. 4 . Material and Energy Balance. : 79–101.
- Mustereț, C.P. & Teodosiu, C. 2007. Removal of persistent organic pollutants from textile wastewater by membrane processes. *Environmental Engineering and Management Journal*, 6(3): 175–187.
- Ojemaye, C.Y. & Petrik, L. 2021. Pharmaceuticals and Personal Care Products in the Marine Environment Around False Bay, Cape Town, South Africa: Occurrence and Risk-Assessment Study. *Environmental Toxicology and Chemistry*: 0–2.
- Padhi, B. 2012. Pollution due to synthetic dyes toxicity & carcinogenicity studies and remediation. *International Journal of Environmental Sciences*, 3(3): 940–955.
- Panda, D. & Manickam, S. 2019. Hydrodynamic cavitation assisted degradation of persistent endocrine-disrupting organochlorine pesticide Dicofol: Optimization of operating parameters and investigations on the mechanism of intensification. *Ultrasonics Sonochemistry*, 51: 526–532. <https://doi.org/10.1016/j.ultsonch.2018.04.003>.
- Panda, D., Saharan, V.K. & Manickam, S. 2020. Controlled hydrodynamic cavitation: A review of recent advances and perspectives for greener processing. *Processes*, 8(2).
- Patients, S., in Solid Cancer, P.C., Hassan, B.A.R., Yusoff, Z.B.M., Othman, M.A.H., Bin, S., information is available at the end of the Chapter, A. & [Http://dx.doi.org/10.5772/55358](http://dx.doi.org/10.5772/55358). 2012. Water Pollution: Effects, Prevention, and Climatic Impact. *Intech*: 13.
- Patil, P.N., Bote, S.D. & Gogate, P.R. 2014. Degradation of imidacloprid using combined advanced oxidation processes based on hydrodynamic cavitation. *Ultrasonics Sonochemistry*, 21(5): 1770–1777. <http://dx.doi.org/10.1016/j.ultsonch.2014.02.024>.
- Peralta, E., Roa, G., Hernandez-Servin, J.A., Romero, R., Balderas, P. & Natividad, R. 2014. Hydroxyl Radicals quantification by UV spectrophotometry. *Electrochimica Acta*, 129: 137–141.
- Pereira, L. & Alves, M. 2012. Dyes-environmental impact and remediation. *Environmental Protection Strategies for Sustainable Development*: 111–162.
- Pramanik, B.K., Pramanik, S.K. & Suja, F. 2015. A comparative study of coagulation, granular- and powdered-activated carbon for the removal of perfluorooctane sulfonate and perfluorooctanoate in drinking water treatment. *Environmental Technology (United Kingdom)*, 36(20): 2610–2617.
- Prambudy, H., Supriyatin, T. & Setiawan, F. 2019. The testing of Chemical Oxygen Demand (COD) and Biological Oxygen Demand (BOD) of river water in Cipager Cirebon. *Journal of Physics: Conference Series*, 1360(1).
- Saharan, V.K., Badve, M.P. & Pandit, A.B. 2011. Degradation of Reactive Red 120 dye using hydrodynamic cavitation. *Chemical Engineering Journal*, 178: 100–107. <http://dx.doi.org/10.1016/j.cej.2011.10.018>.
- Saharan, V.K., Pandit, A.B., Satish Kumar, P.S. & Anandan, S. 2012. Hydrodynamic cavitation

- as an advanced oxidation technique for the degradation of Acid Red 88 dye. *Industrial and Engineering Chemistry Research*, 51(4): 1981–1989.
- Saranraj, P. 2013. Bacterial biodegradation and decolourization of toxic textile azo dyes. *African Journal of Microbiology Research*, 7(30): 3885–3890.
- Saratale, R.G., Saratale, G.D., Chang, J.S. & Govindwar, S.P. 2011. Bacterial decolorization and degradation of azo dyes: A review. *Journal of the Taiwan Institute of Chemical Engineers*, 42(1): 138–157. <http://dx.doi.org/10.1016/j.jtice.2010.06.006>.
- Saravacos, G. & Maroulis, Z. 2007. Process Engineering Economics. In 47–82.
- Shah, Y.T., Pandit, A.B. & Moholkar, V.S. 1999. Energy Efficiency and the Economics of the Cavitation Conversion Process. : 277–312.
- Sharma, S., Ruparelia, J. & Patel, M. 2011. A general review on advanced oxidation processes for waste water treatment. *International conference on current ...*: 8–10. http://nuicone.org/site/common/proceedings/Chemical/poster/CH_33.pdf.
- Sinnott, R.K. 2005. *Chemical Engineering Design*. 4th ed. Oxford: Elsevier Butterworth-Heinemann.
- Surpățeanu, M. & Zaharia, C. 2004. Advanced oxidation processes for decolorization of aqueous solution containing Acid Red G azo dye. *Central European Journal of Chemistry*, 2(4): 573–588.
- Tao, Y., Cai, J., Huai, X., Liu, B. & Guo, Z. 2016. Application of Hydrodynamic Cavitation to Wastewater Treatment. *Chemical Engineering and Technology*, 39(8): 1363–1376.
- Thanekar, P. & Gogate, P. 2018. Application of hydrodynamic cavitation reactors for treatment of wastewater containing organic pollutants: Intensification using hybrid approaches. *Fluids*, 3(4). 1-24.
- Trojanowicz, M. 2020a. Removal of persistent organic pollutants (POPs) from waters and wastewaters by the use of ionizing radiation. *Science of the Total Environment*, 718: 134425.
- Trojanowicz, M. 2020b. Science of the Total Environment Removal of persistent organic pollutants (POPs) from waters and wastewaters by the use of ionizing radiation. *Science of the Total Environment*, 718: 134425.
- USEPA 2017. Technical Fact Sheet - Perfluorooctane Sulfonate (PFOS) and Perfluorooctanoic Acid (PFOA). EPA 505-F-17-001, United States Environmental Protection Agency. (May): 6: 1-8.
- Vítez, T., Ševčíková, J. & Opletová, P. 2012. Evaluation of the efficiency of selected wastewater treatment plant. *Acta Universitatis Agriculturae et Silviculturae Mendelianae Brunensis*, 60(1): 173–180.
- Wang, X.-K., Zhang, S.-Y. & Li, S.-P. 2009. Decolorization of Reactive Brilliant Red K-2BP in Aqueous Solution by Using Hydrodynamic Cavitation. *Environmental Engineering Science*, 26(1).

APPENDIX A

Table 0.1 Table Absorbance measurements and percent decolouration of OR2 using orifice 2 mm diameter hole in the HC pilot plant at an inlet pressure of 300 KPa for 60 min

Time (min)	Sample	Absorbance	% Decolouration
0	200	1,17	0
10	201	0,212	82

20	202	0,0743	94
30	203	0,0528	95
40	204	0,0453	96
50	205	0,0461	96
60	206	0,0395	96

Table 0.2 Absorbance measurements and percent decolouration of OR2 using orifice 3 mm diameter hole in the HC pilot plant at an inlet pressure of 300 KPa for 60 min

Time (min)	Sample	Absorbance	% Decolouration
0	300	1,18	0
10	301	0,120	90
20	302	0,0977	92
30	303	0,0513	96
40	304	0,0555	95
50	305	0,0364	97
60	306	0,0506	96

Table 0.3 Absorbance measurements and percent decolouration of OR2 using orifice 4 mm diameter hole in the HC pilot plant at an inlet pressure of 300 KPa for 60 min

Time (min)	Sample	Absorbance	% Decolouration
0	400	1,24	0
10	401	0,205	83
20	402	0,0935	92
30	403	0,0966	92
40	404	0,0739	94
50	405	0,0404	97
60	406	0,0336	97

Table 0.4 Absorbance measurements and percent decolouration of OR2 using orifice 5 mm diameter hole in the HC pilot plant at an inlet pressure of 300 KPa for 60 min

Time (min)	Sample	Absorbance	% Decolouration
0	500	1,19	0
10	501	0,363	70
20	502	0,485	59
30	503	0,635	47
40	504	0,646	46

50	505	0,774	35
60	506	0,870	27

Table 0.5 Absorbance measurements and percent decolouration of OR2 using orifice 6 mm diameter hole in the HC pilot plant at an inlet pressure of 300 KPa for 60 min

Time (min)	Sample	Absorbance	% Decolouration
0	600	1,20	0
10	601	0,421	65
20	602	0,290	76
30	603	0,555	54
40	604	0,584	51
50	605	0,845	30
60	606	1,86	-54

Table 0.6 Absorbance measurements and percent decolouration of OR2 using venturi the

Time (min)	Sample	Absorbance	% Decolouration
0	V0	1,25	0
10	V1	0,833	34
20	V2	0,578	54
30	V3	0,232	82
40	V4	0,457	64
50	V5	0,695	45
60	V6	0,690	45

Table 0.7 Absorbance measurements and percent decolouration of OR2 + 100 g FeSO₄ using orifice 2 mm diameter hole in the HC pilot plant at an inlet pressure of 300 KPa for 60 min

Time (min)	Sample	Absorbance	% Decolouration
0	2F0	1,18	0
10	2F1	0,0832	93
20	2F2	0,0663	94
30	2F3	0,0476	96
40	2F4	0,0323	97
50	2F5	0,0253	98
60	2F6	0,0686	94

Table 0.8 Absorbance measurements and percent decolouration of OR2 + 100 g FeSO₄ using orifice 3 mm diameter hole in the HC pilot plant system at an inlet pressure of 300 KPa for 60 min

Time (min)	Sample	Absorbance	% Decolouration
0	3F0	1,12	0
10	3F1	0,0787	93
20	3F2	0,101	91
30	3F3	0,0263	98
40	3F4	0,0192	98
50	3F5	0,0380	97
60	3F6	0,0333	97

Table 0.9 Absorbance measurements and percent decolouration of OR2 + 100 g FeSO₄ using orifice 4 mm diameter hole in the HC pilot plant at an inlet pressure of 300 KPa

Time (min)	Sample	Absorbance	% Decolouration
0	4F0	1,21	0
10	4F1	0,302	75
20	4F2	0,138	89
30	4F3	0,126	90
40	4F4	0,138	89
50	4F5	0,0536	96
60	4F6	0,0481	96

Table 0.10 Absorbance measurements and percent decolouration of OR2 + 100 g FeSO4 using orifice 5 mm diameter hole in the HC pilot plant at an inlet pressure of 300 KPa for 60 min

Time (min)	Sample	Absorbance	% Decolouration
0	5F0	1,22	0
10	5F1	0,190	84
20	5F2	0,335	73
30	5F3	0,468	62
40	5F4	0,487	60
50	5F5	0,562	54
60	5F6	0,567	54

Table 0.11 Absorbance measurements and percent decolouration of OR2 + 100 g FeSO4 using orifice 6 mm diameter hole in the HC pilot plant at an inlet pressure of 300 KPa for 60 min

Time (min)	Sample	Absorbance	% Decolouration
0	6F0	1,23	0
10	6F1	0,682	44
20	6F2	0,428	65
30	6F3	0,666	46
40	6F4	0,989	19
50	6F5	1,16	5
60	6F6	0,883	28

Table 0.12 Absorbance measurements and percent decolouration of OR2 + 10 ml H2O2 using orifice 2 mm diameter hole in the HC pilot plant at an inlet pressure of 300 KPa for 60 min

Time (min)	Sample	Absorbance	% Decolouration
0	2H0	0,438	0
10	2H1	0,0994	77,28
20	2H2	0,0916	79,06286
30	2H3	0,0622	85,78286
40	2H4	0,0330	92,45714
50	2H5	0,0302	93,09714
60	2H6	0,0420	90,4

Table 0.13 Absorbance measurements and percent decolouration of OR2 + 10 ml H2O2 using orifice 3 mm diameter hole in the HC pilot plant at an inlet pressure of 300 KPa for 60 min

Time (min)	Sample	Absorbance	% Decolouration
0	3H0	0,787	0
10	3H1	0,113	86
20	3H2	0,118	85
30	3H3	0,0291	96
40	3H4	0,0225	97
50	3H5	0,0409	95
60	3H6	0,0346	96

Table 0.14 Absorbance measurements and percent decolouration of OR2 + 10 ml H2O2 using orifice 4 mm diameter hole in the HC pilot plant at an inlet pressure of 300 KPa for 60 min

Time (min)	Sample	Absorbance	% Decolouration
0	4H0	1,14	0
10	4H1	0,202	82
20	4H2	0,125	90
30	4H3	0,127	89
40	4H4	0,123	89
50	4H5	0,0545	95
60	4H6	0,0392	97

Table 0.15 Absorbance measurements and percent decolouration of OR2 + 10 ml H2O2 using orifice 5 mm diameter hole in the HC pilot plant at an inlet pressure of 300 KPa for 60 min

Time (min)	Sample	Absorbance	% Decolouration
0	5H0	1,12	0
10	5H1	0,147	87
20	5H2	0,0791	93
30	5H3	0,0531	95
40	5H4	0,0567	95
50	5H5	0,520	53
60	5H6	0,0559	95

Table 0.16 Absorbance measurements and percent decolouration of OR2 + 10 ml H2O2 using orifice 6 mm diameter hole in the HC pilot plant at an inlet pressure of 300 KPa for 60 min

Time (min)	Sample	Absorbance	% Decolouration
0	6H0	1,11	0
10	6H1	0,669	40
20	6H2	0,825	26
30	6H3	1,023	8
40	6H4	1,60	-44
50	6H5	1,14	-2
60	6H6	0,946	15

Table 0.17 Absorbance measurements and percent decolouration of OR2 + 100g FeSO4 + 10 ml H2O2 using orifice 2 mm diameter hole in the HC pilot plant at an inlet

Time (min)	Sample	Absorbance	% Decolouration
0	2FH0	0,879	0
10	2FH1	0,182	79
20	2FH2	0,206	77
30	2FH3	0,173	80
40	2FH4	0,127	86
50	2FH5	0,204	77
60	2FH6	0,725	18

Table 0.18 Absorbance measurements and percent decolouration of OR2 + 100g FeSO4 + 10 ml H2O2 using orifice 3 mm diameter hole in the HC pilot plant at an inlet pressure of 300 KPa for 60 min

Time (min)	Sample	Absorbance	% Decolouration
0	3FH0	0,830	0
10	3FH1	0,0899	89
20	3FH2	0,106	87
30	3FH3	0,0423	95
40	3FH4	0,331	60
50	3FH5	0,0132	98
60	3FH6	0,0268	97

Table 0.19 Absorbance measurements and percent decolouration of OR2 + 100g FeSO₄ + 10 ml H₂O₂ using orifice 4 mm diameter hole in the HC pilot plant at an inlet pressure of 300 KPa for 60 min

Time (min)	Sample	Absorbance	% Decolouration
0	4FH0	1,06	0
10	4FH1	0,233	78
20	4FH2	0,144	86
30	4FH3	0,141	87
40	4FH4	0,133	87
50	4FH5	0,0733	93
60	4FH6	0,0428	96

Table 0.20 Absorbance measurements and percent decolouration of OR2 + 100 g FeSO₄ + 10 ml H₂O₂ using orifice 5 mm diameter hole in the HC pilot plant at an inlet pressure of 300 KPa for 60 min

Time (min)	Sample	Absorbance	% Decolouration
0	5FH0	1,08	0
10	5FH1	0,139	87
20	5FH2	0,0804	93
30	5FH3	0,0639	94
40	5FH4	0,0734	93
50	5FH5	0,512	52
60	5FH6	0,519	52

Table 0.21 Absorbance measurements and percent decolouration of OR2 + 100 g FeSO₄ + 10 ml H₂O₂ using orifice 6 mm diameter hole in the HC pilot plant at an inlet pressure of 300 KPa for 60 min

Time (min)	Sample	Absorbance	% Decolouration
0	6FH0	1,24	0
10	6FH1	0,761	39
20	6FH2	1,51	-22
30	6FH3	1,44	-16
40	6FH4	2,45	-98
50	6FH5	2,60	-110
60	6FH6	2,49	-101

Table 0.22 Absorbance measurements and percent decolouration of OR2 using the combination of orifice 2 mm diameter hole and the venturi in the HC pilot plant at an inlet pressure of 300 KPa for 30 min

Time (min)	Sample	Absorbance	% Decolouration
0	2OV0	1,26	0
5	2OV1	0,487	61
10	2OV2	0,241	80
15	2OV3	0,152	88
20	2OV4	0,108	91
25	2OV5	0,0859	93
30	2OV6	0,0732	94

Table 0.23 Absorbance measurements and percent decolouration of OR2 using the combination of orifice 3 mm diameter hole and the venturi in the HC pilot plant at an inlet pressure of 300 KPa for 30 min

Time (min)	Sample	Absorbance	% Decolouration
0	3OV0	1,27	0
5	3OV1	0,289	77
10	3OV2	0,126	90
15	3OV3	0,0713	94
20	3OV4	0,0548	96
25	3OV5	0,0497	96
30	3OV6	0,0523	96

Table 0.24 Absorbance measurements and percent decolouration of OR2 using the combination of orifice 4 mm diameter hole and the venturi in the HC pilot plant

Time (min)	Sample	Absorbance	% Decolouration
0	4OV0	1,26	0
5	4OV1	0,214	83
10	4OV2	0,0862	93
15	4OV3	0,0529	96
20	4OV4	0,0432	97
25	4OV5	0,0425	97
30	4OV6	0,0427	97

Table 0.25 Absorbance measurements and percent decolouration of OR2 using the combination of orifice 5 mm diameter hole and the venturi in the HC pilot plant at an inlet pressure of 300 KPa for 30 min

Time (min)	Sample	Absorbance	% Decolouration
0	5OV0	1,25	0
5	5OV1	0,190	85
10	5OV2	0,0646	95
15	5OV3	0,0480	96
20	5OV4	0,0391	97
25	5OV5	0,0369	97
30	5OV6	0,0393	97

Table 0.26 Absorbance measurements and percent decolouration of OR2 using the combination of orifice 6 mm diameter hole and the venturi in the HC pilot plant at an inlet pressure of 300 KPa for 30 min

Time (min)	Sample	Absorbance	% Decolouration
0	6OV0	1,26	0
5	6OV1	0,362	71
10	6OV2	0,0783	94
15	6OV3	0,0499	96
20	6OV4	0,0467	96
25	6OV5	0,127	90
30	6OV6	0,190	85

Table 0.27 Absorbance measurements and percent decolouration of OR2 using orifice 2 mm diameter hole in the HC pilot plant at an inlet pressure of 300 KPa for 10 min

Time (min)	Sample	Absorbance	% Decolouration
0	200	1,64	0
2	201	0,713	56
4	202	0,412	75
6	203	0,236	86
8	204	0,174	89
10	205	0,170	90

Table 0.28 Absorbance measurements and percent decolouration of OR2 using orifice 3 mm diameter hole in the HC pilot plant at an inlet pressure of 300 KPa for 10 min

Time (min)	Sample	Absorbance	% Decolouration
0	300	1,28	0
2	301	0,708	45
4	302	0,382	70
6	303	0,207	84
8	304	0,150	88
10	305	0,150	88

Table 0.29 Absorbance measurements and percent decolouration of OR2 using orifice 4 mm diameter hole in the HC pilot plant at an inlet pressure of 300 KPa for 10 min

Time (min)	Sample	Absorbance	% Decolouration
0	400	1,53	0
2	401	0,743	52
4	402	0,423	72
6	403	0,267	83
8	404	0,215	86
10	405	0,204	87

Table 0.30 Absorbance measurements and percent decolouration of OR2 using orifice 5 mm diameter hole in the HC pilot plant at an inlet pressure of 300 KPa for 10 min

Time (min)	Sample	Absorbance	% Decolouration
0	500	1,32	0
2	501	0,709	46
4	502	0,415	67
6	503	0,262	80
8	504	0,215	84
10	505	0,198	85

Table 0.31 Absorbance measurements and percent decolouration of OR2 using orifice 6 mm diameter hole in the HC pilot plant at an inlet pressure of 300 KPa for 10 min

Time (min)	Sample	Absorbance	% Decolouration
0	600	1,29	0
2	601	0,848	34
4	602	0,478	63
6	603	0,344	73
8	604	0,268	79
10	605	0,225	83

Table 0.32 Absorbance measurements and percent decolouration of OR2 using venturi in the HC pilot plant at an inlet pressure of 300 KPa for 10 min

Time (min)	Sample	Absorbance	% Decolouration
0	V0	1,51	0
2	V1	1,02	32
4	V2	0,918	39
6	V3	0,770	49
8	V4	0,682	55
10	V5	0,643	57

Table 0.33 Absorbance measurements and percent decolouration of OR2 using the combination of orifice 2 mm diameter hole and the venturi in the HC pilot plant at an inlet pressure of 300 KPa for 10 min

Time (min)	Sample	Absorbance	% Decolouration
0	2OV0	1,54	0
2	2OV1	0,887	43
4	2OV2	0,731	53
6	2OV3	0,487	68
8	2OV4	0,467	70
10	2OV5	0,452	71

Table 0.34 Temperature reading

Time (min)	Temperature (° C)
0	22
2	25
4	27
6	30
8	32
10	34

Table 0.35 Chemical oxygen demand measurements of perfluorooctanoic acid

Time (min)	Sample	COD (mg/l)
0	2Oc0	18
2	2Oc1	35
4	2Oc2	38
6	2Oc3	36
8	2Oc4	33
10	2Oc5	34

APPENDIX B

Table 0.1 Moody chart for determination of friction factor f (Beck & Collins, 2008)

